Diplomarbeit

The Mutational Landscape of Patients with Usher Syndrome in Southern Austria

eingereicht von

Esther Schaiter

zur Erlangung des akademischen Grades

Doktorin der gesamten Heilkunde

(Dr. med. univ.)

an der

Medizinischen Universität Graz

ausgeführt an der

Universitäts-Augenklinik Graz

unter der Anleitung von

Dr. med. univ. Laura Posch-Pertl

Univ.-Prof. Dr. med. univ. Andreas Wedrich

Dr. med. univ. Sarah Verheyen

Graz, am 22.01.2021

Eidesstattliche Erklärung

Ich erkläre ehrenwörtlich, dass ich die vorliegende Arbeit selbstständig und ohne fremde Hilfe verfasst habe, andere als die angegebenen Quellen nicht verwendet habe und die den benutzten Quellen wörtlich oder inhaltlich entnommenen Stellen als solche kenntlich gemacht habe.

Graz, am 22.01.2021 *Esther Schaiter eh.*

Acknowledgments

First, I would like to thank my supervisor Dr. Laura Posch-Pertl for providing guidance and feedback throughout this thesis. Your friendly and supportive manner made working on this project so much more fun.

I would also like to thank Univ.-Prof. Dr. Andrea Wedrich and Dr. Sarah Verheyen for their support throughout this project.

Thanks also to my partner Raphael for proofreading my thesis a thousand times.

I would also like to acknowledge my mother for her support and sympathetic ear.

Table of Content

List of Abbreviations

ADGRV1	Adhesion G Protein-coupled Receptor V1
	Also known as VLGR1
BCVA	Best Corrected Visual Acuity
CIB2	Calcium and Integrin Binding Family Member 2
CDH23	Cadherin Related 23
CLRN1	Clarin 1
dB	Decibel
DHA	Docosahexaenoic Acid
DNA	Deoxyribonucleic Acid
DFNB31	Whirlin
ERG	Electroretinogram
FAF	Fundus Autofluorescence
GCL	Ganglion Cell Layer
HARS	Histidyl-tRNA Synthetase
HL	Hearing Loss
ICD-10	International Classification of Diseases 10th Revision
ILM	Internal Limiting Membrane
INL	Inner Nuclear Layer
IPL	Inner Plexiform Layer
IS	Inner Segment
mRNA	Messenger RNA
MYO7A	Myosin VIIA
N	Nucleus
NFL	Nerve Fibre Layer
NGS	Next Generation Sequencing
OCT	Optical Coherence Tomography
OLM	Outer Limiting membrane
ONL	Outer Nuclear Layer
OPL	Outer Plexiform Layer
OS	Outer Segment
PCDH15	Protocadherin related 15
PCR	Polymerase Chain Reaction

PDZD7	PDZ domain containing 7
RNA	Ribonucleic Acid
RNFL	Retinal Nerve Fiber Layer
RP	Retinitis Pigmentosa
RPE	Retinal Pigment Epithelium
S	Synapse
SANS	USH1 protein network component sans
	Also known as USH1G
SD	Standard Deviation
SFCT	Subfoveal choroidal thickness
SNP	Single Nucleotide Polymorphism
USH	Usher Syndrome
USH1	Usher Syndrome Type 1
USH2	Usher Syndrome Type 2
USH3	Usher Syndrome Type 3
USH2A	Usherin
USH1C	USH1 protein network component harmonin
USH1G	USH 1 protein network component sans
VLGR1	Very Large G-protein-coupled-receptor
	Also known as ADGRV1
WHRN	Whirlin
	Also known as DFNB31

List of Figures

List of Tables

Zusammenfassung

Einleitung – Usher Syndrom (USH) ist eine autosomal-rezessiv vererbte Erkrankung, die zu einer Innenohrschwerhörigkeit und progredientem Sehverlust aufgrund von Retinitis Pigmentosa führt(1,2). Das Ziel dieser Studie ist es, Varianten in den USH-assoziierten Genen und deren Prävalenz in Süd-Österreich zu erfassen. Bonnet et al. 2016 stellte fest, dass in Slowenien die häufigste USH-assoziierte Mutation *USH2A*:c.11864G>A (p.Trp3955*) ist(3). Aufgrund der geographischen Nähe zu Österreich, nehmen wir eine Prävalenz der c.11864G>A Mutation von über 8% in unserer Studienpopulation an.

Methoden – Es wurden 17 Patientinnen und Patienten mit klinisch bestätigtem USH in die Studie eingeschlossen. Mit Hilfe von gezielter Exome-Sequenzierung wurde versucht Mutationen in USH-assoziierten Genen zu identifizieren. Wenn durch diese Untersuchungsmethode keine oder eine Variante auf nur einem Allel entdeckt wurde, wurde noch eine SNP-Array-Analyse durchgeführt, um Kopienzahlveränderungen zu erfassen.

Resultate – Mutationen in zumindest einem Allel wurden in 94.12% (16/17) der Fälle festgestellt. Der Großteil der Varianten wurde in USH2-assoziierten Genen identifiziert: in 76.47% (13/17) im *USH2A* Gen und in 11.76% (2/17) im *ADGRV1* Gen. Die Variante c.11864G>A im *USH2A* Gen konnte bei fünf Studienteilnehmerinnen und Studienteilnehmern (29.4%) auf einem Allel identifiziert werden. Eine homozygote Deletion des Exons 20 des *CDH23*-Gens wurde bei einem Patienten festgestellt.

Diskussion – Nach unserem Wissen ist dies die erste Studie, welche die USH assoziierten Mutationen in USH Patientinnen und Patienten in Süd-Österreich zu erfassen versucht. Die Ergebnisse unterstützen unsere Hypothese, dass die Verteilung und Prävalenz der Mutationen in Süd-Österreich ähnlich ist wie in Slowenien. Die Variante c.11864G>A im *USH2A* Gen ließ sich bei über 8% in einem Allel nachweisen.

Abstract

Introduction – Usher syndrome (USH) is an autosomal recessive disease leading to sensorineural hearing loss and progredient visual loss due to retinitis pigmentosa(1,2). This study aims to identify variants in USH associated genes and their prevalence in southern Austria. According to Bonnet et al. 2016 the most common mutation in USH associated genes in Slovenia is *USH2A*:c.11864G>A (p.Trp3955*)(3). Due to the geographic proximity we assume a prevalence of the c.11864G>A variant > 8% in southern Austria.

Methods – We included 17 patients with clinically confirmed USH in our study. Targeted exome sequencing was used to identify mutations on USH associated genes and modifier genes. If no mutations or a monoallelic mutation was found, SNP array analysis was performed to identify copy number variations.

Results – Mono- or biallelic mutations were detected in 94.12% (16/17) of the cases. The majority of variants was identified in the USH2-related genes: in 76.47% (13/17) in the *USH2A* gene and in 11.76% (2/17) in the *ADGRV1* gene. Five subjects (29.4%) carried the c.11864G>A variant on one allele of the *USH2A* gene. A biallelic homozygous deletion of exon 20 in the *CDH23* gene was found in one subject.

Discussion – To our knowledge this is the first study to assess the mutational landscape of USH patients in southern Austria. Our results support our hypothesis that the mutational landscape in southern Austria is similar to that of Slovenia. The variant c.11864G>A in the *USH2A* gene has a prevalence > 8% in southern Austria.

1. Introduction

Usher syndrome (USH) is a hereditary disease, leading to hearing loss (HL) and visual impairment. USH is the most frequent cause for combined deaf-blindness and accounts for 50% of all cases. The prevalence is estimated to be 3-6 per 100.000. It's a genetically heterogeneous disease, inherited autosomal-recessively(1). Up to date causal mutations in 14 disease associated genes have been described(2). Clinically, USH is characterized by retinitis pigmentosa (RP), a progressive degeneration of the retina, hearing loss and in some cases vestibular dysfunction. Depending on the severity of hearing loss, presence of vestibular dysfunction and age of onset of RP USH is divided into three major clinical types: USH type 1, USH type 2 and USH type 3(1).

USH type 1 is characterized by congenital deafness, vestibular dysfunction and early onset of RP in the first decade of life. USH type 2 is a less severe form, patients show congenital moderate to profound hearing impairment, normal vestibular function and onset of RP during the second decade. USH type 3 is the least common type with variable onset of RP and hearing loss. Vestibular dysfunction can be both present or absent(1).

The most common clinical type is USH type 2, accounting for two-thirds of USH patients, followed by USH type 1, making up one-third. USH type 3 is the rarest form, but it is more common in consanguineous and isolated populations(4).

Of the 13 known USH genes, six are associated with USH type 1 (MYO7A, USH1C, CDH23, PCDH15, USH1G, CIB2); four with type 2 (USH2A, ADGRV1[1], WHRN, PDZD7) and three with type 3 (CLRN1, HARS, ABDH12[2])(2,5,6).

Variants in four additional genes (ARSG, CEP250, CEP78, ESPN) have been associated with USH in case reports, however their pathogenicity remains to be determined(7–10).

Although great progress has been made in the identification of molecular causes of USH, variants in the reported genes of the literature do not explain all USH cases(4).

[1] Formerly known as: VLGR1 or GPR98.

[2] USH associated mutations in the gene ABDH12 have only been identified in a few non-Caucasian families(5).

1.1. Primary Hypothesis and Exploratory Objectives

This study aims to identify variants in USH associated genes and their prevalence in southern Austria. To our knowledge so far, no study has assessed the prevalent mutations in USH patients from this Austrian region. Bonnet et al. 2016 screened 427 USH patients from six European countries including Slovenia and identified variants in 93% of USH cases. The two most common mutations detected in their study were *USH2A*:c.2299delG (p.Glu767Serfs*21) and *USH2A*:c.11864G>A (p.Trp3955*). Analysing the regional distribution of these variants, a high prevalence of the c.11864G4A variant was found in Slovenia(3). Based on the geographic proximity between southern Austria and Slovenia, we assume a prevalence > 8% of the c.11864G4A variant in our USH population.

Our exploratory objectives are to investigate genotype-phenotype correlations, since the relatively broad spectrum of RP onset, progression and severity make an individual prognosis difficult.

1.2. The Eye

The following chapters provide a general overview of the anatomy and the function of the eye and the ear. Particular focus is placed upon the retina and photoreceptors, since they are the primary structures affected by retinitis pigmentosa(11).

The eye is commonly divided into two sections: an anterior and posterior segment. Both segments have different functions. The anterior segment contains the refractive optical system which focuses light on the retina, while the posterior segment is responsible for photoreception. The posterior segment of the eye consists of the vitreous body and three layers called sclera, choroid and retina, while the anterior segment of the eye deviates from this structure. It is composed of the cornea, lens, iris, ciliary body as well as the anterior and posterior chamber(12).

1.2.1. Anterior Segment of the Eye

The anterior segment of the eye contains the refractive system, which is mainly composed of the transparent cornea and the biconvex lens. The cornea has a higher refractive power than the lens since it has a stronger curvature and a higher refractive index(12). The mean refractive power of the cornea is 43 dioptres, while the lens has a lower refractive power of 10 to 20 dioptres(12,13). Although the lens has a lower refractive power it is essential for clear sight, since its shape and therefore also its refractive power can be modified in a process called accommodation (see Figure 1). This allows the eye to see objects clearly at various distances by increasing or decreasing its refractive power(13,14).

Anterior to the lens is the iris, which has a central opening called pupil through which light enters the eye. The size of the pupil is adjustable. It is regulated by smooth muscles located in the iris. This makes it possible to regulate the amount of light entering the eye. Adjacent to the iris is the ciliary body, which contains the muscle which controls the shape of the lens. It also produces a transparent fluid called the aqueous humour which fills the anterior and posterior chamber of the eye. The anterior chamber is located between the cornea and the iris, while the smaller posterior chamber is located behind the iris. The aqueous humour is excreted into the posterior chamber by the ciliary body and flows into the anterior chamber through the pupil. Lens and cornea have no blood supply but obtain nutrients from

the surrounding aqueous humour, respectively the aqueous humour and the tear film(14).

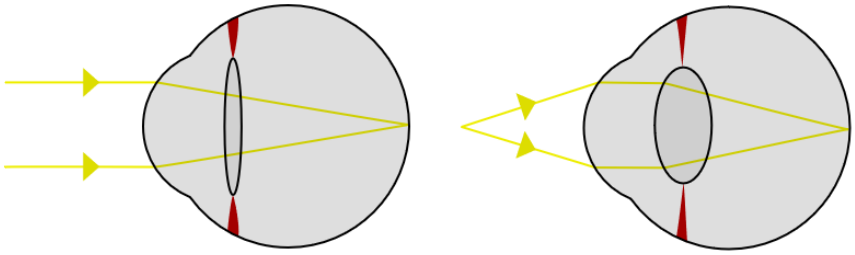

Figure 1: Lens accommodation. Left eye: far point accommodation; Right eye: near point accommodation(15).

1.2.2. Posterior Segment of the Eye

The posterior segment of the eye is composed of three main layers. The outer layer is the sclera, the middle layer is called uvea and the innermost light-sensitive layer is the retina(12). The space inside of the eye is filled by the vitreous body, which is mainly composed of collagen fibres and hydrogel (see Figure 2)(14).

The sclera forms the thick outer layer of the eye, which is mainly composed of collagen fibres. It has a great tensile strength and together with the intraocular pressure it forms the spherical shape of the eye. On its posterior side the sclera has a small opening through which the optic nerve exits the eye together with the central retinal artery and vein(12). Anteriorly the sclera is limited by the corneal limbus which is the junction between the sclera and the cornea(13).

Above the sclera is the uvea, which consists of three parts: the iris, the ciliary body and the choroid. The anteriormost part is the iris, which regulates the size of the pupil. It is attached to the ciliary body, which contains the ciliary muscle responsible for the accommodation of the lens. The posterior part of the uvea is formed by the choroid, a vascular layer which nourishes the outer layers of the retina(13).

The retina forms the inner layer of the eye, which contains light-sensitive photoreceptor cells. They convert light into electrical signals, which can be transferred to the visual cortex of the brain through the optic nerve. This process makes it possible to transmit visual images from the eye to the brain(12). The retina can be divided into a central and a peripheral region. The central retina is quite small. It expands around the fovea, which is a small depression located in the centre of the posterior retina(16,17). The fovea is packed with specialized photoreceptor cells called cones, which provide high-resolution and colour vision(18). In fact, the

fovea is the part of the retina with the highest resolution(17). The region in which the fovea is located is called macula lutea which translates to yellow spot. Its name derives from yellow pigments, which are found in macular neural cells(16). They filter short wavelength light, which is thought to enhance vision and it reduces photooxidative stress(19). On the nasal side of the fovea lays the blind spot (optic disc), which contains no photoreceptor cells since the optic nerve exits the eye at this point together with the central retinal artery and vein. A healthy optic disc has a yellow-orange colour(13,14). The retina outside of the central region forms the peripheral retina and it extends from the central retina to the ora serrata, which is the junction between retina and ciliary body(12,16). This part of the retina mainly contains rod photoreceptor cells, which provide vision in dark environments(18).

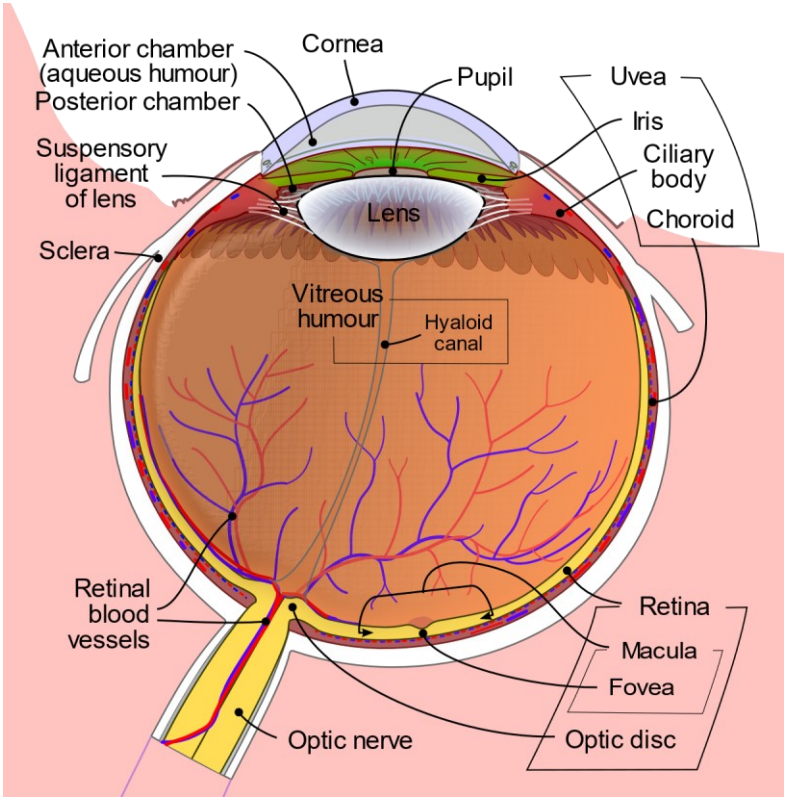

Figure 2: Anatomy of the eye(20).

1.2.3. Retina

The retina is composed of two main stratums: the single-layered retinal pigment epithelium (RPE) and the multi-layered neural retina, consisting of the light-sensitive photoreceptor cells and a system of neural cells(13,21). The neurosensory retina forms the inner stratum facing the vitreous body, while the RPE is the outer stratum, which is attached to the choroid(13). The two adjacent layers are only connected at the ora serrata and optic disc, where the neural retina firmly attaches to the RPE(12). Interactions between both retinal layers are vital for photoreceptor maintenance and proper visual function(22). Indeed, RPE cell dysfunction can lead to secondary photoreceptor cell loss and visual impairment(23).

RPE cells are pigmented cells with microvilli on their apical surfaces. These small membrane protrusions wrap around the outer segments of photoreceptor cells, which may be essential for retinal attachment(23,24). The pigment in the RPE melanosomes absorb scattered light, without it stray light would reduce visual acuity and images would be blurry(21,23). Another important role of the RPE is the phagocytosis of shed photoreceptor outer segments. The outer segments contain light-sensitive visual pigments. After they have been activated, they are insensitive to light. The RPE recycles these inactivated pigments, which plays an important role for the normal functioning of the visual cycle and outer segment renewal(23).

The neural retina instead consists of several different neural cells. The outer layer (facing the RPE) is composed of light-sensitive photoreceptor cells. They are the first neurons of the visual pathway. Their electrical responses to light are transmitted to the second neurons of the visual pathway called bipolar cells. These cells connect to ganglion cells, which compose the third neuron. The axons of the ganglion cells run towards the optic disc where they join to form the optic nerve, which exits the eye. So, the neural retina contains the first three neurons of the visual pathway. All further neural connections lay outside of the eye(21,25).

In addition to photoreceptors, bipolar cells and ganglion cells the neural retina contains two other types of neurons, namely horizontal and amacrine cells. Horizontal cells provide lateral connections between bipolar and photoreceptors cells, while amacrine cells synapse with bipolar and ganglion cells. These additional neural connections in the retina make it possible to process visual information before it is transmitted to the brain(21,25).

1.2.4. Retinal Layers

Histologically the retina can be divided into ten layers. While each layer is clearly recognisable in histological preparations, not all of them are independent functional units. This chapter describes the histological layers in the same order as light passes through the retinal layers (see Figure 3)(21,26).

- Internal limiting membrane (ILM) – border between retina and vitreous body formed by Müller cells (retinal glial cells)
- Nerve fibre layer (NFL) – axons of the ganglion cells
- Ganglion cell layer (GCL) – cell nuclei of retinal ganglion cells
- Inner plexiform layer (IPL) – synapses between bipolar, ganglion and amacrine cells
- Inner nuclear layer (INL) – nuclei of bipolar cells, horizontal cells, amacrine cells and Müller cells
- Outer plexiform layer (OPL) – synapses between photoreceptor cells and bipolar cells as well as horizontal cells
- Outer nuclear layer (ONL) – nuclei of photoreceptor cells
- Outer limiting membrane (OLM) – cell junctions between photoreceptor cells and Müller cells
- Inner segments (IS) and outer segments (OS) of photoreceptor cells
- Retinal pigment epithelium (RPE)(21,26)

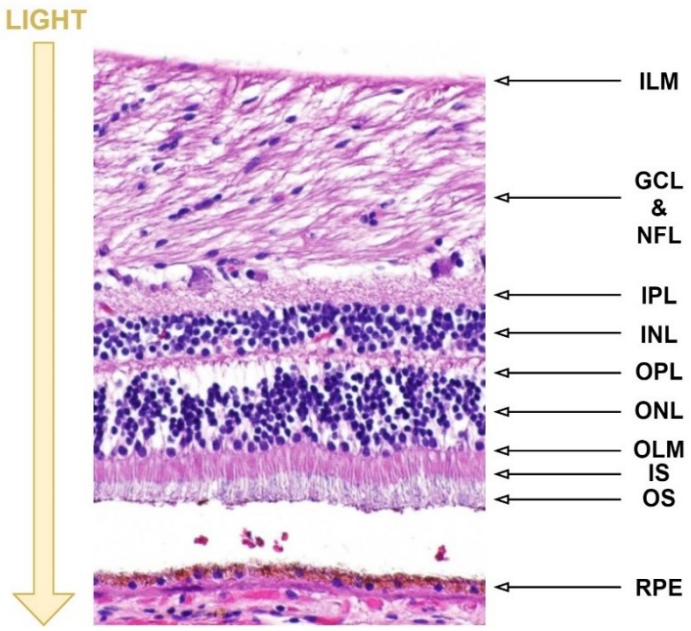

Figure 3: Cross-sectional histological preparation of the retina(27).

1.2.5. Photoreceptors

Photoreceptors are light-sensitive sensory cells capable of phototransduction, which is the process of converting light stimuli into electrochemical signals(13,28). Humans have two different types of photoreceptor cells, which differ in their shape, distribution and function. Based on their shape they are called rods and cones (see Figure 4)(16,18). Each human eye contains approximately six million cones and 126 million rods(13). Rod photoreceptor cells are more light-sensitive than cones. They mediate vision in dark environments (scotopic vision), while cones provide high-acuity colour vision in daylight conditions(18). Cones are mainly located in the central retina in particular in the macular region, while rods dominate in the peripheral retina(16).

Although rods and cones have a different morphology, their basic structure is the same. They consist of a light-sensitive outer segment, an inner segment and a short axon. The outer segments are filled with visual pigments, which allow light perception. Cones integrate their visual pigments in plasma membrane invaginations, while rods store them in plasma membrane discs(21). Rods contain a visual pigment called rhodopsin, while cones have different types of visual pigment(29). There exist three different types of cones, each containing a different visual pigment with different absorption maxima(12). The three cone types are either sensitive to red, green or blue light which allows colour perception(13).

The outer segments are constantly renewed. New discs are formed at the proximal end of the outer segment and pushed towards the apex, where old discs are shed and phagocytosed by the RPE. Components for the disc renewal are produced in the inner segment and then transported to the outer segment through the connecting cilium(30). The inner segment is the metabolic centre of the photoreceptor cell, it contains all cell organelles, like mitochondria and ribosomes, except the cell's nucleus, which either lies at the junction between inner segment and axon or in the axon(12,21). The photoreceptor's axon emerges from the inner segment and ends in the synaptic terminal, where it is interconnected with the second neuron(21).

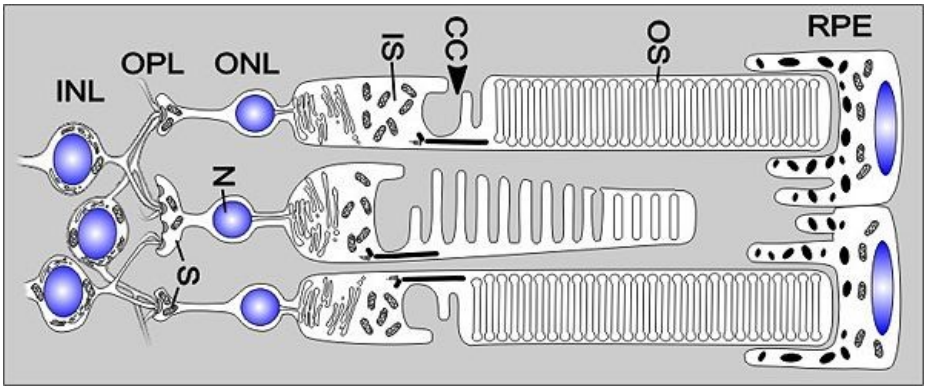

Figure 4: Rod and cone photoreceptor cells. Abbreviations: Nucleus (N), Synapse (S)(31).

1.3. The Ear

The ear is our organ of hearing and balance. It is composed of the outer ear, the middle ear and the inner ear, which contains the two sensory organs(12).

The outer ear consists of two main parts. The visible part of the outer ear is formed by the auricle, which is composed of elastic fibrocartilage and a thin layer of skin, which largely lacks subcutaneous fat (except for the ear lobe). It collects the soundwaves and directs them into the non-visible part of the outer ear, which is the external ear canal(32,33). A cartilaginous process of the auricula forms the outermost part of the tube-shaped ear canal, which extends inward until it reaches the eardrum. The outer two-thirds of the canal are made of cartilage, while the inner third is made of bone(12,33). The inner surface of the ear canal is covered with epithelium. Similar to the auricula the skin of the ear canal is tightly attached to the perichondrium or periosteum. The cartilaginous part of the ear canal contains different glands. Their secretion and desquamated epithelial cells produce the cerumen also known as earwax(21,32).

The ear canal ends at the ear drum or tympanic membrane, which divides the outer and middle ear. It is a thin oval membrane composed of two parts: a larger and ticker part called pars tensa and a smaller one called pars flaccida, which is located in the upper quadrants of the ear drum(32,34). The pars tensa consists of three layers. The outer layer (facing the ear canal) is covered with the same epithelium as the ear canal, the middle layer is composed of elastic and collagenous fibres and the inner layer (facing the middle ear) is covered with mucosa(21,34). In contrast to the pars tensa the pars flaccida lacks the middle fibrous layer(32,34).

The eardrum can be evaluated by using an otoscope. A healthy eardrum has a greyish colour, is translucent and it shows a light reflex, when light hits the membrane during otoscopic examination(34). In the centre of the membrane behind the pars tensa the first ossicle becomes visible(32,34).

The middle ear is composed of a small cavity called the tympanic cavity, the mastoid air cells and the auditory tube. The tympanic cavity is a narrow space located behind the eardrum, which forms its lateral wall. The medial border is formed by the oval and the round window, which separate the middle ear and the inner ear. The auditory ossicles called malleus, incus and stapes are located in the tympanic cavity. They form a chain reaching from the eardrum to the oval window, which makes it possible to transmit the sound vibrations from the ear drum to the inner ear. On the ventral side of the tympanic cavity lays the opening of the auditory tube, which connects the middle ear with the pharynx. This connection allows the ventilation of the air-filled tympanic cavity and it helps to regulate the pressure in the middle ear. In contrast to the outer ear, the middle ear is covered by mucosa(12,33).

The inner ear contains the two sensory organs of the ear(12). It is embedded in the bony labyrinth which is a system of fluid-filled cavities formed by the temporal bone(21,33). The fluid filling the bony labyrinth is called perilymph. In it flows the membranous labyrinth, which is composed of several ducts and sacs. The membranous labyrinth contains the sensory epithelia of the inner ear and it is filled with a viscous fluid termed endolymph(12,21).

1.3.1. Inner Ear

The bony and the membranous labyrinth compose the inner ear (see Figure 5), which can be divided into three major parts: the vestibulum, the vestibular system and the cochlea. The vestibulum is located behind the oval window. It forms the central section of the bony labyrinth and it contains the two otolith organs called utricle and sacculus, which detect translational head movements and the position of the head(12,35). The posterior wall of the vestibulum opens into the three semicircular canals, which compose the vestibular system together with the otolith organs. Each semicircular canal expands at the junction to the utriculus to form the ampullae, which contain sensory epithelium. While the otolith organs are able to detect linear acceleration, the semicircular canals detect angular acceleration. Both systems contain ciliated sensory cells. Their cilia are embedded in a gelatinous

mass. Movement accelerates this mass, causing the cilia to bend. Analogous to the eye, where light stimulates the photoreceptors, the bending of the cilia is the stimulus for the vestibular organ(12,21).

The cochlea which contains the organ of hearing is located anterior to the vestibulum. It is a spiral-shaped tube, which turns around a central axis made of bone. The inside of the cochlea can be divided into three compartments. The one in the middle called scala media contains the sensory cells. Above the scala media runs the scala vestibuli and beneath it lays the scala tympani. The scala vestibuli and tympani are both filled with perilymph and the two perilymphatic spaces meet at the apical end of the cochlea. The scala media instead is filled with endolymph. It is separated from the scala vestibuli and tympani by the basal membrane and the Reissner's membrane(12,36). The organ of hearing also called organ of Corti is located on the basal membrane. It consists of a system of supporting cells and sensory cells, which convert mechanical displacement into nerve impulses. The Corti-organ contains two types of sensory cells called inner and outer hair cells, since they have stereocilia on their apical end. The hair cells are covered by a jellylike mass called the tectorial membrane, that the longest stereocilia of the hair cells reach into(21,36).

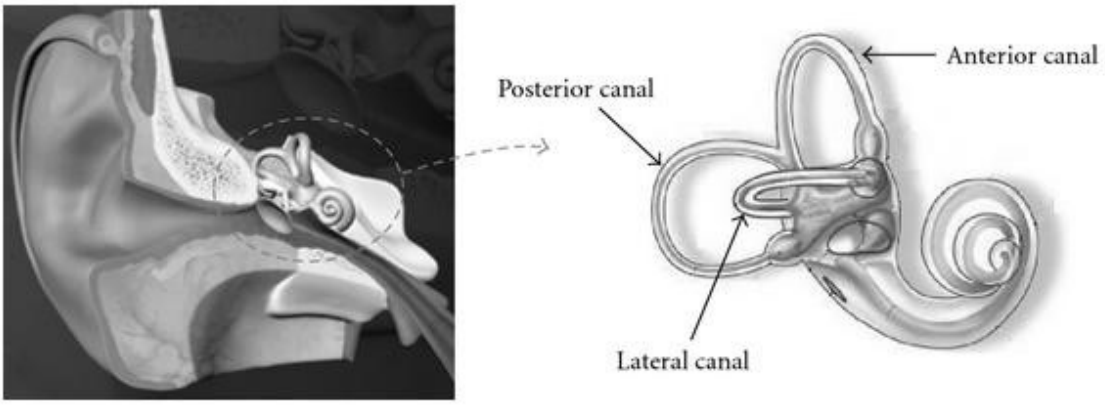

Figure 5: Anatomy of the inner ear(37).

1.3.2. Hair Cells and Pathologies of Hair Bundle Development

The human Corti-organ contains two types of sensory cells called inner and outer hair cells(21). Both cell types have stiff protrusions on their apical side called stereocilia(21,38). These protrusions are the mechanically sensitive part of the hair cells. They make it possible to convert mechanical movements into electrical signals

(mechanotransduction), and therefore to detect sound(39). While hair cells have hair bundles on their apical side, their synaptic connections are located on the basal side(12).

Each hair cell has several stereocilia on its apical side, which are organized into hair bundles(21,38). The stereocilia have different lengths and the longest even reach into the tectorial membrane. The tips of these stereocilia are connected through extracellular filaments called tip links. They are mainly formed by the proteins cadherin 23 and protocadherin 15(21,39). Both proteins probably play an important role in hearing, since they seem to be involved in mechanoelectrical transduction. Test animals with mutations in the genes encoding for cadherin 23 or protocadherin 15 often showed abnormal mechanoelectrical responses. In humans mutations in these genes are associated with USH, which causes syndromic hearing loss(40).

While links between stereocilia are important for the cohesion of adult hair bundles, they also play an important role in hair bundle development. During hair cell development several transient links are formed between their adjacent stereocilia. In mice for example transient lateral links and ankle links at the base of stereocilia are formed. They gradually diminish and are fully absent in adult mice, while tip links are still present throughout adulthood. Besides cadherin 23 and protocadherin 15 there are other proteins involved in the formation of these links. Usherin and VLGR1 (Very large G-protein-coupled-receptor 1) for example might be present in transient ankle links. The dysfunction or lack of these proteins is also associated with USH(4).

1.3.3. The Physiology of Hearing

This chapter explains the basic concepts of hearing. Sound perception is made possible by the organ of Corti, which converts sound into nerve impulses that can be transferred to our brain. Sound is created by sound waves which are pressure waves traveling through different mediums like air or fluids. Humans are capable of detecting sound waves between 20 and 20.000 Hz, but as we age our range of detectable sound frequencies decreases. Low frequency sounds are sensed as deep sounds, while high frequencies are perceived as high-pitched sounds. Loudness on the other hand depends on the amplitude of the sound wave and is measured in decibels (dB). The human ear hears sounds between 0 dB and 130 dB(33,41).

The human outer ear collects sound waves and directs them into the external ear canal. Once the pressure waves have reached the tympanic membrane, they set the membrane in motion causing it to vibrate. The vibrations of the eardrum are then transmitted to the ossicles of the middle ear. They are passed from the malleus to the incus and finally the stapes, which attaches to the oval window and transmits the vibrations onto the perilymph. This way sound waves are transmitted from the outer to the inner ear (see Figure 6)(33,41).

The vibrations passed on by the ossicles generate a pressure wave in the perilymph, which travels along the scala vestibuli and scala tympani until it reaches the round window. This pressure wave causes the scala media which contains the Corti-organ to bend towards the scala tympani. These pressure-induced displacements cause a slight shift between the basal and tectorial membrane, which in turn causes stereocilia that reach into the tectorial membrane to bend. The bending of stereocilia induces the opening of mechanoelectrical transduction channels of hair cells, which causes them to depolarize. When inner hair cells depolarize, they release a neurotransmitter at their synapse which activates the postsynaptic neurons. While inner hair cells convert sound waves into electrical signals, the outer hair cells are responsible for sound amplification(41,42).

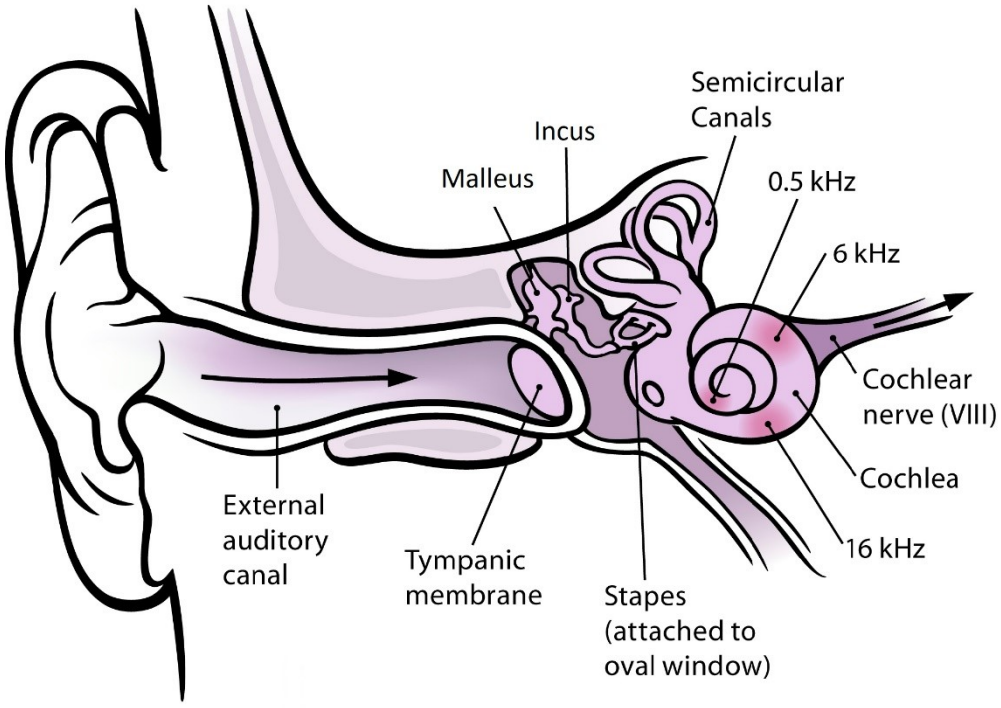

Figure 6: The path of sound waves through the ear(43).

1.4. Usher Syndrome: Clinical Manifestation

USH is a heterogeneous disorder. The cardinal symptoms of USH are vision and hearing loss, but the severity of symptoms may vary considerably among patients. USH is commonly divided into three clinical types: USH type 1, USH type 2 and USH type 3. Patients are classified by the degree and progression of hearing impairment and by the presence of vestibular dysfunction. Although not all cases can be categorized in this classification, it is still in clinical use(1).

All three clinical types suffer from progressive peripheral vision loss caused by retinitis pigmentosa (RP)(1). Initially patients often complain of night blindness and as the disease progresses, they slowly start to notice the peripheral vision loss. In the end stage of RP, patients are often left with a small central visual field (tunnel vision), but they also might go totally blind(11).

Although the clinical manifestation of USH differs among the three clinical types regarding the severity of hearing loss and vestibular symptoms, all USH types have RP(1). It is controversial whether visual symptoms differ between USH types. More severe visual symptoms, like more restricted visual fields and poorer visual acuity, have been reported in USH type 1 patients. Yet studies show diverging results(44). For example, Edwards et al. came to the conclusion that USH type 1 patients have more severe visual symptoms than USH type 2 patients(45). While Tsilou et al., which conducted a study with 67 USH type 1 and 2 patients, reported no statistically significant differences between the two types. They concluded that the visual symptoms among USH patients vary less than previously reported(44).

1.4.1. Clinical Usher Types

This chapter discusses the clinical manifestation of the three USH types and the differences among them.

USH type 1 is the most severe clinical subtype and it is characterized by congenital deafness. Affected children are born deaf or with profound bilateral, non-progressive hearing loss. If they don't receive a cochlear implant, development of intelligible speech is often not possible. In addition, USH type 1 patients suffer from vestibular dysfunction, which may lead to balance problems and delayed motor development in affected children(1,4,44).

USH type 2 is the most common clinical USH type, accounting for about two-third of all USH cases(3). This clinical type is less severe than USH type 1, since USH

type 2 patients have no vestibular symptoms and only moderate to severe hearing loss(1,40). The hearing impairment in USH type 2 patients remains stable over time and is usually more pronounced in high frequencies(4). Due to the less severe auditory symptoms USH type 2 patients usually develop intelligible speech(44).

USH type 3 is the rarest USH type, accounting for only 2-4% of all USH cases. Although its worldwide prevalence is relatively low, USH type 3 is found more frequently among isolated populations[3], where it may account for up to 40% of all USH cases(1). Clinically USH type 3 is the most heterogeneous type, with variable onset of RP and variable onset of hearing loss(1,4). Vestibular symptoms may be present or absent, either way USH type 3 patients usually show normal motor development(1). In contrast to USH type 1 and 2, hearing loss in USH type 3 patients is non-congenital and progressive. Initially auditory symptoms are comparable to USH type 2, with moderate hearing loss in low frequencies and severe hearing loss in high frequencies, but in many USH type 3 patients the hearing loss will progress to profound hearing loss eventually(4).

1.5. Retinitis Pigmentosa

USH is characterized by progressive vision loss due to retinitis pigmentosa(1). The term RP describes a heterogeneous group of inherited retinal dystrophies(46). These different types of retinal degeneration can be non-syndromic or syndromic. Non-syndromic forms are limited to the eyes, with no other organs affected, while syndromic disorders are associated with other systemic symptoms. The most common syndromic RP is USH(11).

RP is characterized by progressive visual field defects and retinal pigment deposits, which can be seen in fundus examination. The disease primarily affects photoreceptors and RPE cells resulting in progressive retinal degeneration(11,46). RP primarily affects rods, leading to night blindness and progressive visual field defects. However, ultimately RP often also involves cones. The exact mechanism by which RP leads to cone loss is unclear. As soon as RP involves cones, central vision is increasingly diminished. Due to its progressive nature, RP can eventually lead to severe visual impairment or even blindness(11,47).

[3] USH type 3 has a high prevalence in Finland and among the Ashkenazi Jewish population(1).

1.5.1. Prevalence and Heredity

Worldwide the number of people living with RP is estimated to be over three million people(48), with a prevalence of 1 in 4000 people in Europe. Genetically the disorder is remarkably heterogenous, with over 60 genes associated with non-syndromic RP(49).

Depending on the causative gene, non-syndromic RP follows different inheritance patterns: autosomal-dominant, autosomal-recessive and X-linked recessive. Other inheritance patterns like mitochondrial or digenic inheritance are quite rare and only account for a very small percentage of RP cases. Expressiveness of RP usually shows no preference regarding ethnicity or gender, except for X-linked recessive RP which is only expressed in males(50). However, the mode of inheritance for some genes influences the age of onset, the rate of disease progression as well as the severity of visual symptoms. Recessive X-linked inheritance for example is associated with rapid disease progression and often leads to total blindness in the third or fourth decade of life(51).

Generally non-syndromic RP is more common than syndromic RP, and among the syndromic forms USH is the most frequent one(49), accounting for 10-30% of all autosomal-recessive RP cases(50). Opposite to non-syndromic RP, USH is inherited mainly[4] autosomal-recessive, with an estimated 3-6 cases per 100.000(4).

1.5.2. Morphology

RP leads to several morphological changes in the retina. Usually these changes affect both eyes and can be seen in fundus examination. Typical fundus manifestations are retinal pigmentary changes (most often bone-spicule and pigment clumpings), attenuation of retinal vessels and a pale waxy optic disc (see Figure 7 and 8)(11).

Retinal pigment deposits are among the most prominent features of RP. They look like black intraretinal spots and have a bone-spicule like shape, which is why they are also called bone-spicule deposits. These dark deposits are often seen in advanced disease stages and are formed by RPE cells, which migrate into the neurosensory retina in reaction to photoreceptor cell death(52).

[4] New data questions USH being inherited strictly autosomal-recessive and considers other inheritance patterns to be possible(106).

These pigment deposits are typically found in the peripheral retina, but they might also be missing, especially in early disease stages. While they are a common feature, they are not mandatory, and their amount does not always correlate with the severity of the disease(11,52).

While bone-spicule deposits, thin retinal vessels and pale optic discs are commonly seen in advanced disease stages, these changes might be absent in early stages. Fundus examination may even seem normal at an early stage, but as the disease progresses, photoreceptor loss and retinal atrophy becomes more notable(11). Retinal atrophy is not only visible in fundus examination, but also evident in cross-sectional images or histological specimen. The progressive loss of photoreceptor cells leads to the thinning of the outer retinal layers and as a result, patients with advanced RP often have a remarkably thin outer nuclear layer. In contrast to the outer layers, the inner retinal layers (inner nuclear layer and ganglion cell layer) seem to remain intact for a long time(52).

Figure 7: Fundus photograph of a patient with RP. The image shows typical signs of RP like thin retinal vessels and pigment deposits(53).

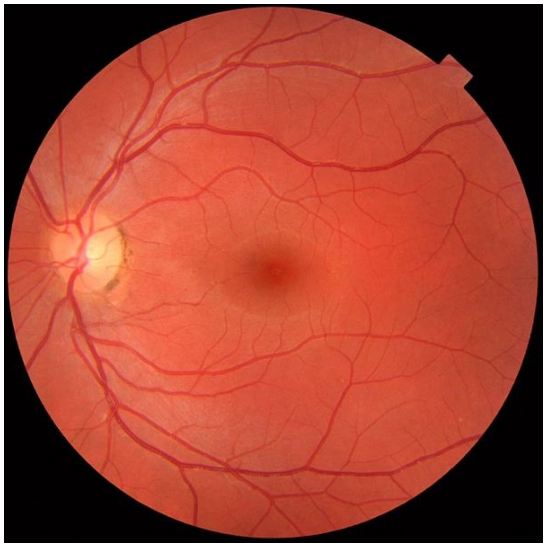

Figure 8: Normal fundus photograph(54).

1.5.3. Symptoms

RP is a retinal dystrophy, which affects both eyes and causes progressive vision loss. It is a slowly progressive disease, symptoms develop gradually, and the retinal degeneration evolves over several decades. In fact, most RP patients never go totally blind(11). Typical RP (rod-cone degeneration) primarily affects rod

photoreceptor cells, which are specialised for night vision(11,52). Therefore, the first symptoms of RP are night blindness and problems with dark adaption. Yet patients may not notice their reduced night vision, because artificial lights brighten our night-time environment sufficiently for them to see normally(52). The age of onset of night blindness and visual loss varies highly among RP patients. Some already experience symptoms in their early childhood or in their teenage years, while others may not be affected until later in life(11,52).

Although night vision is reduced early on, vision in broad daylight is usually unimpaired in the earlier disease stages. Initially patients have normal colour vision and visual acuity, provided that no other eye defects are present(11,52).

As disease progresses, visual field defects become more apparent. Patients start to notice their visual field loss in day light, as they step into everyday objects or have difficulties when driving. Usually the visual field defect (scotoma) starts in the mid periphery of the retina and expands towards the macula and outer periphery(11). Initially patients are able to compensate their visual defects quite well, but as the visual field diminishes spatial orientation becomes more difficult(14).

In the end stages of RP patients have lost most of their peripheral vision. They are left with a small range of vision around their fixation point(11) and only see objects they directly look at. This condition is known as tunnel-vision. At this stage spatial awareness or autonomous movement are usually not possible anymore. Yet patients may still be able to read at such advanced disease stages, given their central retina is spared(11,14).

Photophobia is often present in RP patients and is often a cause of great reduced quality of life. This should be considered when adapting spectacles. In later stages, cone dysfunction may lead to diminished central vision, decreased colour discrimination and reduced contrast sensitivity(11). Reduced contrast sensitivity may cause poor subjective eyesight in patients with normal high contrast visual acuity(52).

Many patients with RP are myopic and some even highly myopic which adds additional risk for decreased visual acuity. Further many RP patients are prone to develop cataract earlier than in the normal population. A known complication of RP is macular oedema. It is unclear why RP patients develop oedema. In order to reduce macular oedema, carbonic anhydrase inhibitors are given(11).

In conclusion, it can be said that the clinical manifestation of RP is highly variable. The age of onset, the progression rate as well as the clinical endpoint may differentiate substantially between patients suffering from RP(52).

1.5.4. Diagnosis

The diagnosis of RP is based on medical history, family history and slit lamp examination, imaging, electroretinography and genetic testing. This chapter discusses the most common clinical tests, which are routinely performed to diagnose and follow-up RP patients(55).

Practitioners should assess their patients' medical history including their age of onset and their family history(11,55). RP patients often have a positive family history, so it may be useful to make a detailed pedigree chart(51).

Typical symptoms patients may report in early RP stages are night blindness and photophobia(11). Although night blindness is one of the first symptoms of RP it is often ignored by patients, because artificial night-time lighting is often bright enough to allow vision with cones. As the disease progresses, visual field loss becomes more apparent. Yet patients may experience no subjective difficulties with daily tasks, even though their visual field is significantly reduced. At the time patients become aware of the symptoms, loss of rod function may already be extensive. Therefore, objective testing of photoreceptor function and visual field limits is much more reliable for diagnosis and disease grading than symptoms alone(52).

One of these tests, which allow an objective assessment of photoreceptor function, is the electroretinogram (ERG). It measures the electrical responses of photoreceptor cells, after they have been stimulated with light. In RP patients rod responses are usually decreased(55). These abnormal ERG responses are present before any fundoscopic or visual changes are notable(56) which makes the ERG an essential tool in early RP diagnosis(11).

Slit lamp examination shows typically changes, which are retinal pigmentary changes, attenuation of retinal vessels and a pale waxy optic disc. These changes are not mandatory, but most patients present with at least two of these characteristics(11).

Optical coherence tomography (OCT) is a very useful quick non-invasive and widely available imaging technique to monitor RP patients. OCT scans of patients with RP typically show a loss of the ellipsoid zone and the external limiting membrane, which

is suggestive of photoreceptor loss. Further macular oedema can be monitored easily by OCT(57,58).

Another important imaging technique to monitor RP progression is fundus autofluorescence (FAF), which depicts the presence and distribution of fluorophores mainly lipofuscin in the RPE. RP patients show abnormal FAF images early on with hypofluorescent lesions in the periphery again suggesting photoreceptor loss(59).

In addition to these clinical examinations molecular screening and the assessment of the inheritance pattern are useful for differential diagnosis(47).

1.5.4.1. Age of Onset

The age of onset describes at which age a person first experiences symptoms of RP. It does not refer to the onset of retinal degeneration, since that may start much earlier. This has been demonstrated by ERG examinations, which displayed photoreceptor degeneration in children of age six, even though some remained asymptomatic until much later in life. Therefore, the age of onset is not suitable for measuring disease severity and provides no information on the beginning of retinal degeneration. Moreover, the subjective perception of symptoms varies highly among patients and some might not report symptoms during earlier disease stages(52).

Although the age of onset is unsuitable for measuring the extend of retinal degeneration, it may help with differential diagnosis. The age of onset varies highly among different RP forms. First symptoms may appear in early childhood, adolescence, young adulthood or adulthood(47).

Alternatively, the age of onset can be roughly divided into early and late onset RP. While early onset RP typically becomes apparent in the first decade of life, late onset RP is characterized by onset around or after midlife(11).

1.5.4.2. Visual Acuity

The term visual acuity describes the capacity of the eye to resolve detail. A patient's visual acuity is usually measured by using test charts, which display standardized letters or symbols. The test can be performed with (best corrected visual acuity) or without refractive correction. In retinal diseases usually best-corrected visual acuity is used(60).

In the human eye high spatial resolution is mediated by cone photoreceptor cells(18), which is why the visual acuity is usually unimpaired in the earlier stages

of RP(51,52). Retinal degeneration caused by RP usually starts in the mid-periphery of the retina and primarily affects rod photoreceptor cells(11). But as the retinal degeneration progresses it might also affect the central retina and cause a decline in visual acuity(11,51). However, bad eyesight may also be present at earlier disease stages or it can be a result of complications like cataracts or macular oedema(51). Such complications are quite common among individuals with RP(11). Macular oedema for example has an estimated prevalence of 10-50% among patients with RP(55).

Besides evaluating visual acuity, it might also be useful to assess the contrast sensitivity with a contrast chart. Reduced contrast sensitivity is often present before a decline in visual acuity, but it may lead to poor subjective eyesight(51,52).

1.5.4.3. Perimetry

The visual field is the portion of our surroundings that we are able to see during steady fixation of our eye and head. Our monocular visual field expands about 140 degrees horizontally and 110 degrees vertically. The visual acuity is best in the central visual field and decreases towards the periphery(61). Although, the outer parts of our visual field have low visual acuity, they are essential for daily tasks like walking or driving. Since peripheral vision allows us to detect motion and to see objects without directly looking at them(61,62).

Patients with RP show characteristic changes in their visual fields as the retinal degeneration progresses, which makes perimetry (visual field testing) an essential examination for the diagnosis and monitoring of disease progression of RP. There exist several methods to assess changes or defects (scotomas) in a patient's visual field(55). This chapter will briefly explain a test called Goldmann perimetry, which is the gold-standard to observe visual field changes over time in RP patients(63). To perform this test, the patient is seated in front of a hollow hemispheric bowl called the Goldmann perimeter. Then the patient is asked to fixate the fixation point at the centre of the bowl. After that a small dot of light is projected onto the inner surface of the bowl and then moved towards the centre of the perimeter. This way the test light is moved from outside the visual field into the patient's visual field. The position at which the patient first notices the test light, marks the outer edge of the visual field(61,63). By using different light targets and by positioning the test light at

different locations, this method allows the testing of the peripheral and the central visual field(61).

Visual field testing in patients with RP usually shows progressive peripheral vision loss. In early RP stages patients develop ring-like scotomas in the mid-periphery of the retina. Then as the retinal degeneration progresses the visual field defects spread towards the far periphery as well as the central retina. End stage RP patients are often left with a small central visual field, also known as tunnel vision (see Figure 9)(55,64).

Visual field testing is an important tool to diagnose and stage RP, and to evaluate the level of care a patient needs(55).

Figure 1: Left: Normal binocular vision in day light; Middle: Depiction of peripheral vision loss; Right: Tunnel vision, only a small island of vision is left around the fixation point.

1.5.4.4. Electroretinogram

The Electroretinogram (ERG) is an electrophysiologic test, which allows an objective evaluation of retinal function by measuring light-induced electrical changes of the retina(52,65). When light reaches the light-sensitive photoreceptor cells of the retina it induces various biochemical processes, which trigger a signalling pathway which ultimately results in the hyperpolarization of the photoreceptor cell membrane(21). These electrochemical responses of photoreceptor cells to light provide the basis for the ERG(52,65). The ERG records these light-induced electrical potential changes of the eye at the corneal surface by using a corneal contact lens electrode or conjunctival electrodes(66).

The electrical responses are evoked with different light stimuli. Using stimuli, which differ in light-intensity, colour and frequency, makes it possible to test the rod and cone system independently(47,65). Rod photoreceptor cells are very light-sensitive. They allow vision at low light levels and quickly saturate in a bright environment(65). Therefore, the rod-system is tested in the dark by using a single flash of dim light(52,66). The less light-sensitive cone-system instead is evaluated in the light-

adapted state (rods are saturated), by using flickering white lights(52,65). It's also possible to record the combined responses of rod and cone photoreceptor cells, but the individual evaluation of both systems may help to find out whether the retinal degeneration primarily occurs in the rod or in the cone system(47,52).

The electrical responses recorded by the ERG consist of two main components: the negative a-wave and the positive b-wave(65). The a-wave reflects the light-induced hyperpolarisation of photoreceptor cells, while the b-wave represents the depolarization of bipolar cells. The amplitudes of these waves correlate with retinal function and they are usually reduced in patients with RP(52). ERG examinations of patients in early RP stages typically show reduced rod responses as well as reduced combined responses. As the disease progresses the cone responses decrease too and eventually retinal electrical activity becomes unrecordable(51).

ERG examinations play an important role in the diagnosis and early detection of RP(11,52). Abnormalities are not only detectable in advanced disease stages but are already present at subclinical stages and may be measurable during early childhood. Children that are suspected of developing RP are usually tested at age seven or eight, if they show normal photoreceptor responses at that age RP can be ruled out(52).

1.5.4.5. Optical Coherence Tomography

Optical Coherence Tomography (OCT) is a non-invasive imaging technique, which is frequently used to examine the retina(52,67). The method works similar to ultrasound imaging, but instead of using sound waves it uses light waves to create high-resolution images(67,68). The high-definition of the OCT scans allows the clinician to evaluate the morphology of the retina and to assess any structural changes(52,57). OCT images are cross-sectional images, which makes it possible to measure the thickness of the retina and to identify and evaluate the individual retinal layers or the choroid(67).

Therefore, OCT images are commonly used to assess posterior segment diseases, particularly to evaluate macular pathologies(52,67). In patients with RP OCT images are used to evaluate retinal thickness, to asses changes in the photoreceptor layer and to detect complications of RP like macular oedema(52). Scans of patients with RP usually show an attenuated ellipsoid zone, corresponding to the photoreceptor layer as well as thinning of the external limiting membrane. These changes seen in

OCT scans of patients with RP reflect the photoreceptor degeneration and they correlate with the patient's visual function and visual fields. In fact, the visual field seems to shrink linearly with the thickness of the ellipsoid zone. In contrast to the outer retinal layers the inner retinal layers, including the INL and the ganglion cell layer, remain intact(57).

As the OCT makes it possible to identify these microstructural retinal changes, it is widely used to diagnose retinal diseases and for close monitoring of disease progression and therapy response(67).

1.5.4.6. Fundus Autofluorescence Imaging

Fundus autofluorescence (FAF) is a non-invasive imaging method, which is used to assess the health of the retina and RPE(59,69). The imaging technique records specific molecules in the retina called fluorophores. These molecules generate autofluorescence by absorbing light of a specific wavelength and emitting it at a longer wavelength. FAF captures the emitted light by using different imaging systems like fundus cameras or scanning laser ophthalmoscopes. These imaging systems measure the density of retinal fluorophores to create a density map, which represents the distribution of the autofluorescent molecules in the retina(59).

The eye contains several fluorophores, but FAF imaging is mainly based on a single fluorophore called lipofuscin(59,70). This autofluorescent molecule is located in the RPE, where it accumulates as a byproduct of lysosomal digestion of photoreceptor OS(69,70). The intensity of the autofluorescent signal on FAF images is mainly determined by the amount of accumulated lipofuscin. A higher lipofuscin concentration amplifies the signal intensity (hyper-autofluorescence), while a lower lipofuscin amount results in hypo-autofluorescence(59).

Abnormalities in FAF images are also found in patients with RP(52,59). A common finding seems to be a hyper-autofluorescent ring around the fovea(59,71), which according to Popović et al. may separate functioning from non-functioning retina(71). Corresponding OCT images revealed extensive photoreceptor damage outside of the hyper-autofluorescent ring, while the retina within the ring seemed to be unaffected(59).

1.5.5. Management of Patients with RP

Currently there exists no cure for RP[5]. Therefore, this chapter will provide an overview about the experimental therapy approaches for RP and the current management of patients with RP(51,72).

Therapy approaches that have been considered in the past are nutritional supplements as well as hyperbaric oxygen therapy. Several nutritional supplements like vitamin A, vitamin E or docosahexaenoic acid (DHA) have been tested in clinical trials, but they showed little to no therapeutic benefit. High-dose vitamin A supplementations with 15.000 IU/day seemed to slow down the reduction of ERG amplitudes in patients with RP, but had no effect on their visual acuity or visual field(52,64). Since the benefits of high-dose vitamin A seem to be minimal and because vitamin A may cause severe adverse effects like liver damage it is not recommended. In some genetic RP subtypes it may even lead to worsening of the retinal function(51). In contrast to vitamin A supplementation, the daily intake of vitamin E seemed to have a negative effect on disease progression(73). The last nutritional supplement mentioned in this chapter is DHA. It is an essential fatty acid, which is present in multiple body tissues including the retina. In fact photoreceptors have the highest levels of DHA of all body cells and DHA deficiencies may disturb photoreceptor cell function and lead to vision impairment(74). In patients with RP DHA supplementation seemed to have positive effects on visual field sensitivity, but it did not slow disease progression. Similar to some nutritional supplements long term hyperbaric oxygen therapy showed some therapeutic benefits. Hyperbaric oxygen therapy reduced vision loss in patients with RP, but it wasn't capable of stopping the decline in visual acuity(64). In conclusion none of the mentioned therapy approaches were able to slow the retinal degeneration in RP(52,64).

Although disease progression cannot be stopped, the management of patients with RP should include regular follow-up appointments. Yearly visits allow the clinician to assess disease progression and to treat any RP related complications, which may compromise vision(11,51). Posterior subcapsular cataracts for example are quite common in patients with RP and may cause impaired vision, which can be removed with cataract surgery(52,72). Another treatable complication which may cause

[5] Although the first gene therapy for LCA has been approved in 2017, gene therapy currently remains an experimental treatment for most RP types(75).

vision loss is macular oedema. It can be treated with carbonic anhydrase inhibitors(51,52).

These regular visits should also be used to inform the patients about new treatment options and to introduce them to rehabilitation programs or supportive patients' associations. If needed the patients should also be brought into contact with social services or get psychological help, in particular after disease announcement or loss of central vision(11,51). Patients may also benefit from genetic counselling, which may improve their understanding of RP(11,51).

The clinician should also check for any refractive errors in patients with RP since their correction might lead to improvements in the patient’s eyesight(52). Specifically, patients should be made aware of the possibility of light filters and polarisation to reduce photophobia and may increase contrast by blocking light of specific wave lengths. Patients with RP may also benefit from other visual aids like magnifying glasses or electronic reading devices(51,52). Furthermore, patients with RP are advised to wear sunglasses outdoors which block wave lengths up to 550 nm to protect their retina from photic damage(11,51,72).

Currently there is no treatment that is able to slow or even stop disease progression for USH patients. Research is currently focusing on treatments to slow or stop retinal degeneration. These include gene therapies, stem cell treatments as well as the administration of neuroprotective factors. But these therapies might only be of benefit in earlier disease stages, when there are still vital photoreceptor cells in the retina. In advanced disease stages other approaches like retinal implants are needed. Even though these therapies are still being developed, they seem to be promising future treatments and they will be discussed in the following chapters(72).

1.5.6. Gene Therapy

This chapter provides a basic understanding of gene therapy, since gene therapy might be a promising therapeutic approach for monogenic retinal diseases like USH(75).

Disease-causing mutations can be divided into two major types: loss-of-function and gain-of-function mutations. While loss-of-function mutations cause defective or missing proteins, gain-of-function mutations lead to the production of harmful proteins. Although gene therapy might be a good approach for both types, different therapeutic strategies are needed for them(52,75,76).

For example, if a recessive disease is caused by a loss-of-function mutation, the patients cells have two non-functioning copies of a gene. So, the therapeutic approach is to add a normal copy into the patients cells(76). This way the transcriptional machinery of the cell can use the normal gene copy to produce the missing protein. A gain-of-function mutation instead leads to the assembly of a harmful gene product(75). Therefore, the goal is to supress the expression of the abnormal, toxic gene product by modifying a gene's DNA directly or by destroying its mRNA transcripts. This process is called gene silencing(52,76). Although gene therapy may use different approaches, the basic idea is to modify the patients genome to achieve a therapeutic benefit(77,78).

To get the modifying factor (DNA/RNA) into the retinal cells, special gene delivery tools are needed. One commonly used method for gene delivery is the viral vector, for example adeno-associated virus or lentivirus vectors(77). These viral vectors transfer the therapeutic gene to its destination by infecting the target cells(79). To efficiently access the retinal cells, the viral vector is brought in close contact with them either by injecting a vector suspension into the subretinal space (between photoreceptors and RPE) or by injecting it into the vitreous cavity(75).

In general, the eye is particularly suited for gene therapy since the posterior segments are easy to reach through intraocular injections and because of the compartmentalized structure of the eye, which allows specific tissue targeting. Moreover, the blood-retina barrier minimizes any immune response to the administrated foreign material and the systemic dissemination of the drug. Since inherited retinal disorders usually affect both eyes symmetrically, the contralateral, non-treated eye can be used as a control to evaluate the therapeutic outcome(75,77). However recent studies have shown that antibodies may be produced, which reduce the effect of an injection for the contralateral eye. Thus, it is recommended to inject both eyes within a short period of time(80).

The first gene therapy for the eye was voretigen neparvovec (Luxturna ®). It was approved by the FDA in 2017. Luxturna ® is a gene supplementation therapy for RP and LCA-patients[6], which have a mutation in the *RPE65* gene. Affected individuals have insufficient levels of RPE65, a protein involved in the visual cycle. Without this

[6] Leber's congenital amaurosis (LCA)

protein rod photoreceptor cells eventually lose their ability to react to light. The gene therapy has improved the visual function of patients with non-syndromic RP and LCA(75).

Besides the approved therapy for patients with *RPE65* mutations, there are many more gene therapies in development for ocular diseases(75). Currently UshStat, a gene therapy for USH type 1B, is tested in humans to name but one example (ClinicalTrials.gov Identifier: NCT01505062). UshStat is a viral vector, which delivers *MYO7A* to the RPE and photoreceptors. Its subretinal injection led to myosin VIIa expression in test animals lacking a functional *MYO7A* gene and reduced their photoreceptor cell loss. The subretinal drug administration in test animals was well tolerated, had a very low immune response and was limited to the administered compartment, so that the first human clinical trial of UshStat was initiated(81).

1.5.7. Stem Cell Therapy

Gene therapy seems to be a promising therapy approach for early RP stages, but as the disease progresses more and more photoreceptor cells are lost, and the treatment benefit of gene therapy diminishes(77). But since the inner retinal layers are not affected by RP and stay intact even at advanced disease stages, another treatment strategy could be the replacement of lost photoreceptor cells with stem cells in such cases(77,82).

Stem cells are undifferentiated cells, which are capable of self-renewal and to differentiate into specialized cell types (see Figure 10)(83). Currently different sources of stem cells are used in cell replacement studies, such as induced pluripotent stem cells and embryonic stem cells(82). Induced pluripotent stem cells are somatic cells deriving from the patient, which are reprogrammed into pluripotent stem cells by using transcription factors(83,84). Since they can be taken directly from the patient, they are more immunocompatible than embryonic stem cells and pose less ethical issues than the use of embryonic tissue(77,82). But on the other hand, patient derived cells contain the disease-causing mutations, which must be removed before autologous cell replacement therapy. This problem was solved by Burnight et. al., which were able to correct the cell's disease-causing mutations in induced pluripotent stem cells by using CRISPR-Cas9 mediated genome editing(82).

At the moment one major challenge remains the reconstruction of neural connections. Stem cell treatment is therefore more advanced in the replacement of RPE cells than photoreceptor cells, since they are not dependent on synaptic connections to function(77,85). In fact, RPE cells derived from embryonic stem cells have already been tested in patients with retinal dystrophies. The clinical trials conducted by Schwartz et al. reported no major adverse effects associated with stem cell transplantation and even recorded improvements in visual acuity in some patients(77,86). In conclusion it can be said that stem cell replacement of lost RPE cells seems to be a feasible future treatment approach, while the transplantation of photoreceptors seems to be more challenging and is currently still limited to animal models(77).

In the future, the replacement of lost RPE and photoreceptor cells with induced pluripotent stem cells might restore vision in patients with RP to some extent(77,87). In contrast to gene therapies, stem cell treatments would be mutation-independent and therefore they could be applied to a larger spectrum of retinal degenerations. The successful integration of stem cells into the host retina and the restoration of synaptic connections however remain significant challenges(77).

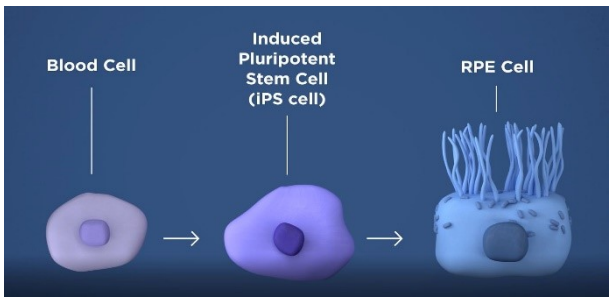

Figure 10: Induced pluripotent stem cell and its differentiation into an RPE cell(88).

1.5.8. Electronic Retinal Implants

RP causes continuous degeneration of the retina(52). Although cell loss occurs in all retinal layers, the degeneration primarily affects rod photoreceptor cells. The inner retinal layers instead are largely spared(52,89). Since some inner neurons remain viable, they can be stimulated with small electrodes, which is the underlying concept of most retinal implants(72,90). They attempt to replace the function of the lost photoreceptor cells by stimulating the remaining neural cells(90). Currently several implants are being developed (cortical visual prosthesis, supra-choroidal

implant, epiretinal and subretinal implants). This chapter introduces two of them, namely subretinal and epiretinal implants(72).

Subretinal implants are light-sensitive microchips, which are implanted under the transparent retina. They are placed in the small space between the RPE cell layer and the neurosensory retina, where the lost photoreceptors were located(72,91). These light-sensitive implants work analogous to photoreceptor cells. When light reaches the retina, the implant outputs small currents that are proportional to the light intensity. This generated electrical signal then simulates the preserved secondary neurons. Zrenner et al. implanted such subretinal implants in three patients suffering from hereditary retinal dystrophies. Prior to their surgery all patients were blind, but after recovery all of them regained some visual perception. For example, they were able to detect bright objects placed on a dark background. One could even identify certain objects like fruits or distinguish different shades of grey(91).

Epiretinal implants instead are built quite differently. They need additional external devices, because they bypass retinal image analysis(91). These implants consist of an external video camera, a video processing unit and an intraocular implant which is placed on the inner retinal surface(72,92). The external camera is attached to a pair of glasses, which the patient can wear. It records a video feed, which is send to the video processing unit in real time. The processing unit reduces the image resolution and transforms the visual information into stimulation patterns. After processing the data is sent to the intraocular implant, which consists of multiple electrodes. These electrodes generate small brightness-dependent currents which stimulate the remaining neurons(92). Epiretinal implants (Argus II) were implanted by da Cruz et al. in 29 patients suffering from RP. They reported that many patients were able to identify letters and some even identified words after surgery(93).

In the last decades great progress has been made in the development of electronic retinal implants. In Europe the first retinal implant namely the Argus II system was approved in 2011. While they make it possible to restore limited visual perception in blind patients, they are far from providing natural eyesight and more research needs to be done(90,93).

1.6. Hearing Loss

Hearing loss (HL) is the most common sensory impairment in humans. According to the WHO approximately 466 million people worldwide suffer from HL. By definition individuals suffering from HL are not capable to detect sounds below 25 dB, while people with normal hearing have a hearing threshold of 20 dB or better(94,95). HL can be categorized by its severity into mild, moderate, moderately severe, severe and profound HL. If the quietest sound an individual can perceive ranges between 26 to 40 dB it is called mild HL. The hearing threshold of individuals with moderate HL lays between 41 to 55 dB and in individuals with moderately severe HL between 56 to 70 dB. People suffering from severe HL have a hearing threshold of 71 to 90 dB and if the hearing threshold is over 90 dB it is called profound HL. To put these numbers into perspective the volume of a normal conversational speech is about 50 to 60 dB(96).

The causes of HL are manifold and can be divided into two major categories: congenital HL (e.g. genetic disorders, infections during pregnancy like rubella or birth asphyxia) and acquired HL (e.g. infectious diseases, chronic ear infections or injuries)(94,95). HL caused by genetic disorders can be further divided into non-syndromic HL and syndromic HL, which accounts for 30% of the genetic cases of HL. In syndromic HL the hearing impairment is associated with other clinical features such as eye, kidney or musculoskeletal anomalies. The most common syndromes leading to HL are USH and Pendred syndrome(95).

HL can also be categorized by the site of the pathology into conductive, sensorineural and mixed HL. Conductive hearing loss is caused by lesions of the outer or middle ear, while sensorineural hearing loss is caused by inner ear or retrocochlear pathologies(97).

1.6.1. Hearing Loss in Usher Syndrome

USH is characterized by hereditary sensorineural hearing loss caused by defective USH proteins, which disrupt the development, maintenance and function of hair cells in the cochlea(40,95). Patients with USH type 1 and type 2 usually experience bilateral, non-progressive congenital HL. While the hearing impairment in patients with USH type 1 is often severe to profound, it might be less severe in patients with USH type 2 (moderate to severe). Usually patients with USH type 2 have better hearing in low frequencies than high frequencies. In contrast to USH type 1 and 2,

USH type 3 is characterized by progressive HL of variable onset. It usually starts before the third decade of life and often progresses to profound HL(4,95).

1.6.2. Diagnosis and Therapy of Hearing Loss

Hearing loss (HL) in children is one of the most common birth defects(95). It is often caused by genetic factors. In fact, about fifty percent of all cases are caused by genetic disorders. Other causes of HL among children are perinatal infections or teratogen exposure, prematurity as well as chronic recurrent otitis media. Determining the aetiology of HL is important for developing a personalized therapeutic approach. Furthermore, it is essential to diagnose HL as early as possible to ensure proper growth and language development in the infant(95,98).

Screening tests used on new-borns are objective hearing tests, which do not rely on the cooperation of the tested individual. The most commonly used tests in infants are the auditory brainstem response and the otoacoustic emissions. Behavioural tests can be used on older children aged 5 or older, who can respond to sound stimuli and follow instructions. Furthermore a detailed medical and birth history as well as family history should be assessed in infants with pathological hearing tests(98).

The management of HL in infants and children depends on the origin of HL and whether the HL is conductive or sensorineural. Depending on the severity of the hearing impairment patients suffering from SNHL can be treated conservatively using hearing aids or through the surgical implantation of a cochlear implant. Either way a long term monitoring of the child to follow its linguistic and social development is necessary(98).

1.7. Usher Syndrome: Genetic Findings

This chapter provides a basic understanding about the genetics of USH. The inheritance pattern and the disease-causing mutations are discussed as well as genetic testing and the different genetic subtypes. But before describing those concepts, a few technical terms shall be explained.

The human DNA (deoxyribonucleic acid) is our hereditary material. It is made up of four chemical bases, which are aligned along a DNA strand. The order of the four bases forms a code, which holds all the instructions our bodies need for development and functioning(99,100).

Specific sequences of these bases are called genes. Some genes encode information to make proteins, while others are made up of noncoding DNA(101). The USH genes for example encode for a variety of different proteins, which are found in the eye and in the ear(102). But even protein-coding genes contain regions of noncoding DNA (introns), which are cut out of the DNA strand before the protein is made. This process is called RNA splicing. The remaining, protein-coding regions are called exons (see Figure 11)(83).

Humans have two copies of each gene, one inherited from the mother and one from the father. These two copies of the same gene are called alleles. The bases at the same genomic position of the two different alleles can be the same or they can differ. If a mutation affects both copies of the gene at the same position, it is called a „homozygous mutation“. If a mutation affects only one allele, it is called „heterozygous“, and if two mutations at different positions in the gene affect the two alleles it is called „compound-heterozygous“(83,101).

The DNA is stored in our cells, where it is tightly packed into bigger units called chromosomes. Human cells mostly have two sets of chromosomes, one paternal and one maternal set. In total we have 23 pairs of chromosomes, one pair of sex chromosomes (which differ between the sexes) and 22 pairs of autosomes(100).

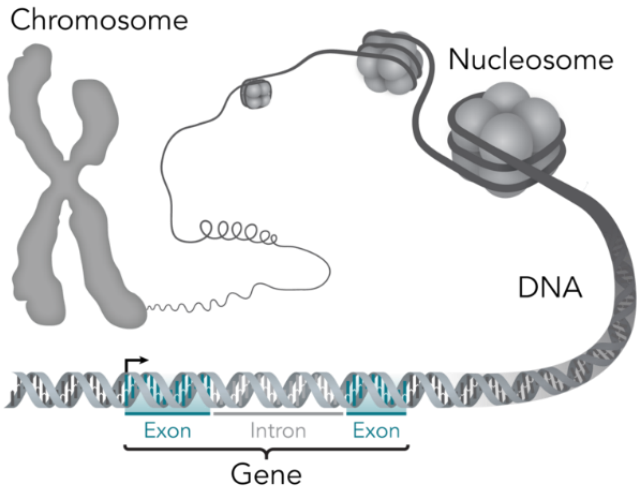

Figure 11: Structure of the DNA(103).

1.8. Autosomal Recessive Inheritance

USH is a disorder caused by genetic alterations (mutations), which are inherited in an autosomal recessive pattern(50). The term autosomal refers to the location of the disease-causing mutations on the autosomes (non-sex chromosomes)(104). Therefore, autosomal inherited diseases usually show no preference regarding gender, females and males can be affected or can be carriers of the disease(50).

A recessive disease only occurs if both copies (alleles) of a gene carry a mutation. So, to have an autosomal recessive illness like USH, an individual must inherit one mutated allele from each parent. An affected person can either carry two identical (homozygous) or two different (compound heterozygous) disease-causing mutations affecting both alleles. Children of consanguineous parents have more and larger homozygous genetic regions and a subsequent increased risk of autosomal recessive diseases(83).

Individuals carrying one normal allele and one mutated allele at the respective gene locus are called heterozygous carriers and are not affected by the disease. However, they can still transmit the single mutated allele to their children. Statistically two parents carrying a heterozygous mutation have following chances with each pregnancy: a 25% chance that their child will inherit two mutated alleles and suffer from USH, a probability of 50% that the child will be non-affected and a 25 % chance that the child is not even a carrier of the disease (see Figure 12)(50,83).

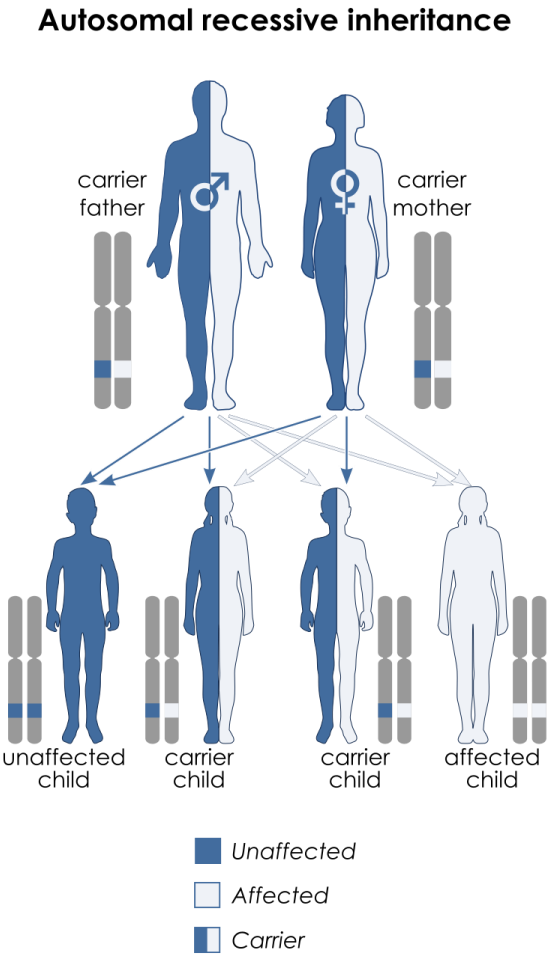

Figure 12: Autosomal recessive inheritance pattern(105).

1.9. Digenic Inheritance

USH has long been considered a monogenic disease. Therefore, an individual would only suffer from the disorder, if it carries two disease-causing mutations in the same gene. But recent data challenges this view, since a few cases of digenic inheritance have been reported(106,107). For the manifestation of a digenic disorder the affected individual must carry two different disease-associated mutations on different genes(108).

Regarding USH, so far only the genetic subtype USH 2C is known to be inherited digenic, the causal variants reported in *PDZD7* and *ADGRV1*. *PDZD7* also functions as a modifier gene in patients with USH type 2A, where it might alter retinal disease expression, since test animals with a mutation in this modifier gene showed an increased retinal cell death. This could indicate a more rapid retinal disease progression in patients with combined mutations in the USH genes and *PDZD7*(106).

Digenic inheritance of USH has also been described in an Italian USH patient, who was heterozygous for mutations in two USH genes. The patient inherited a mutation in *MYO7A* from the unaffected mother and a second mutation in *USH2A* from the unaffected father(109).

Although USH is a predominately monogenic disease, additional inheritance patterns, like digenic or oligogenic inheritance, could explain the great variability of retinal disease expression(109,110).

1.10. Gene Mutations

USH is caused by biallelic changes of the DNA sequence in one of 13 known disease-associated genes(2,111). Those permanent changes are called gene mutations and they can be divided into two major categories: hereditary and acquired mutations.

Hereditary mutations are alterations that are present in the mother's egg or the father's sperm cell. So, when the egg and the sperm fuse to form a fertilized egg, the resulting embryo carries the altered DNA in all of its cells (since all cells derive from the one fertilized egg). Therefore, hereditary mutations are passed down to a child from one or both parents and are present since birth in every cell in the body(111). USH for example is caused by hereditary mutations(2).

Acquired mutations instead are not present since birth but happen at some point after conception. Such mutations can be caused by several factors, like radiation or errors during DNA replication and they are only inheritable, if they also occur in egg or sperm cells of an affected person(111).

While gene mutations can be categorized as above, they can also be classified by their effect on the DNA sequence or their effect on protein expression. The following section explains the main types of mutations that alter the DNA sequence (see Figure 13). These include:

- Deletions: one or more DNA bases are removed from the DNA strand.
- Insertions: one or more DNA bases are added to the DNA strand.
- Substitutions: one or more DNA bases are replaced by one or more different bases.
- Duplications: a segment of DNA is repeated one time in a row(112,113).

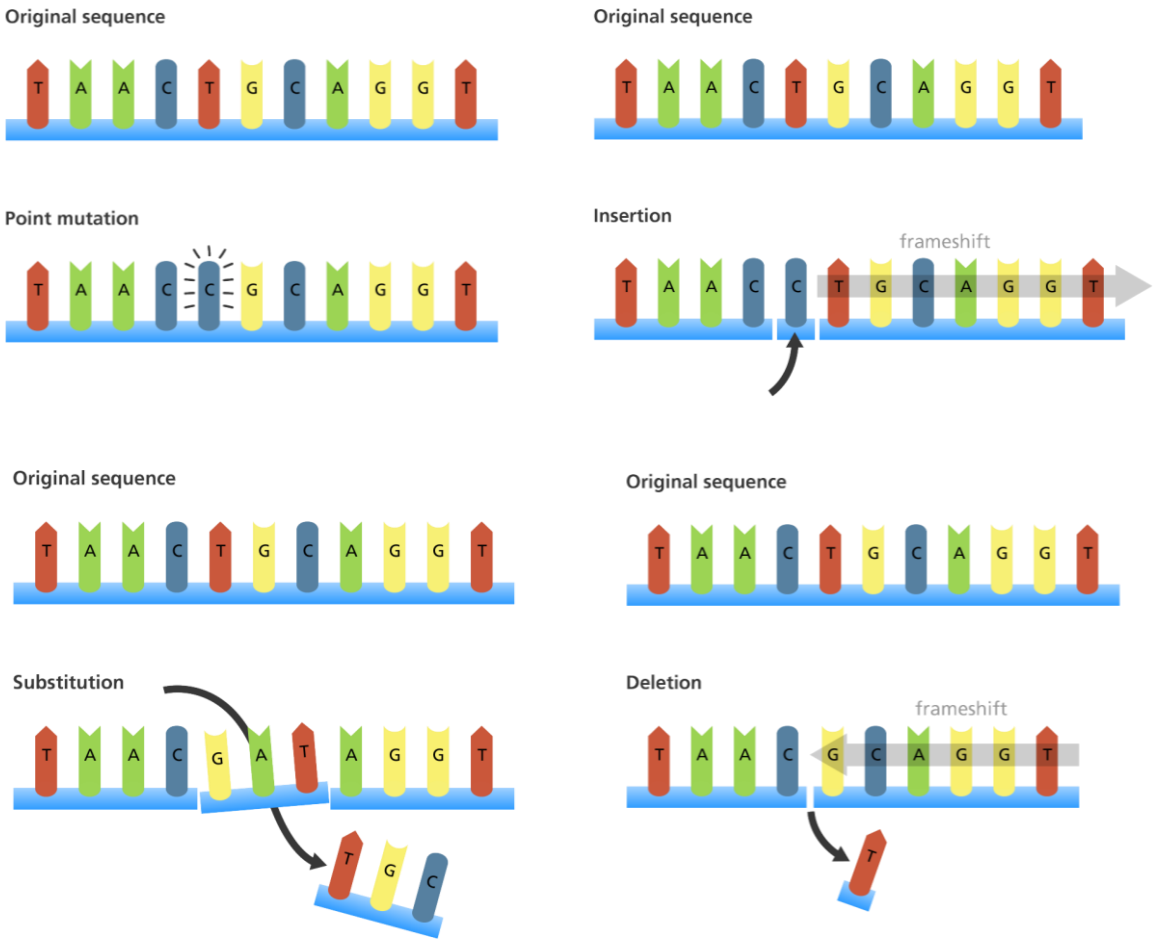

Figure 13: How mutations affect the DNA sequence(114).

Splice site mutations are changes in the DNA sequence in the intron-exon junction. Mutations in these DNA regions can disrupt the splicing process and may lead to an incorrect mRNA synthesis(115).

The last topic covered in this chapter is the effect of variants in a gene on protein expression. Genetic variants do not always change the structure or function of the encoded protein. Therefore, they have varying effects on our health. Some variants have no effects at all and are therefore called silent mutations, while others are harmful and may cause severe illnesses. The clinical consequence of a variant is determined by several factors, one of these outcome-modifying factors is the location of the variant in the coding region of a gene(113,115).

Single base substitutions for example can cause silent, nonsense or missense mutations, depending on the base change and their location in the coding DNA (see Figure 14). Silent mutations, as mentioned above usually do not affect our health, since the mutated DNA still codes for the correct amino acid. Therefore, the encoded

protein is not defective. Missense mutations lead to the substitution of an amino acid with a different amino acid. This change in the amino acid sequence may lead to the assembly of a malfunctioning protein. Like missense mutations, nonsense mutations often result in the production of a faulty protein. Nonsense mutations create stop signals (stop codons) in the DNA sequence, which signal the cell to prematurely terminate the protein synthesis. The resulting proteins are often shortened or non-functioning. A nonsense mutation may also lead to a nonsense mediated decay of the protein(113,115).

While substitutions often lead to an alteration in the amino acid sequence, deletions and insertions often result in a change of a gene's reading frame. Such mutations are called frameshift mutations. Normally three DNA bases code for a specific amino acid. So, a change in the grouping of these bases, by adding or removing one of the three bases, results in a shift of the reading frame. Frameshift mutations often result in a non-functional protein and/ or a premature stop codon(113,115).

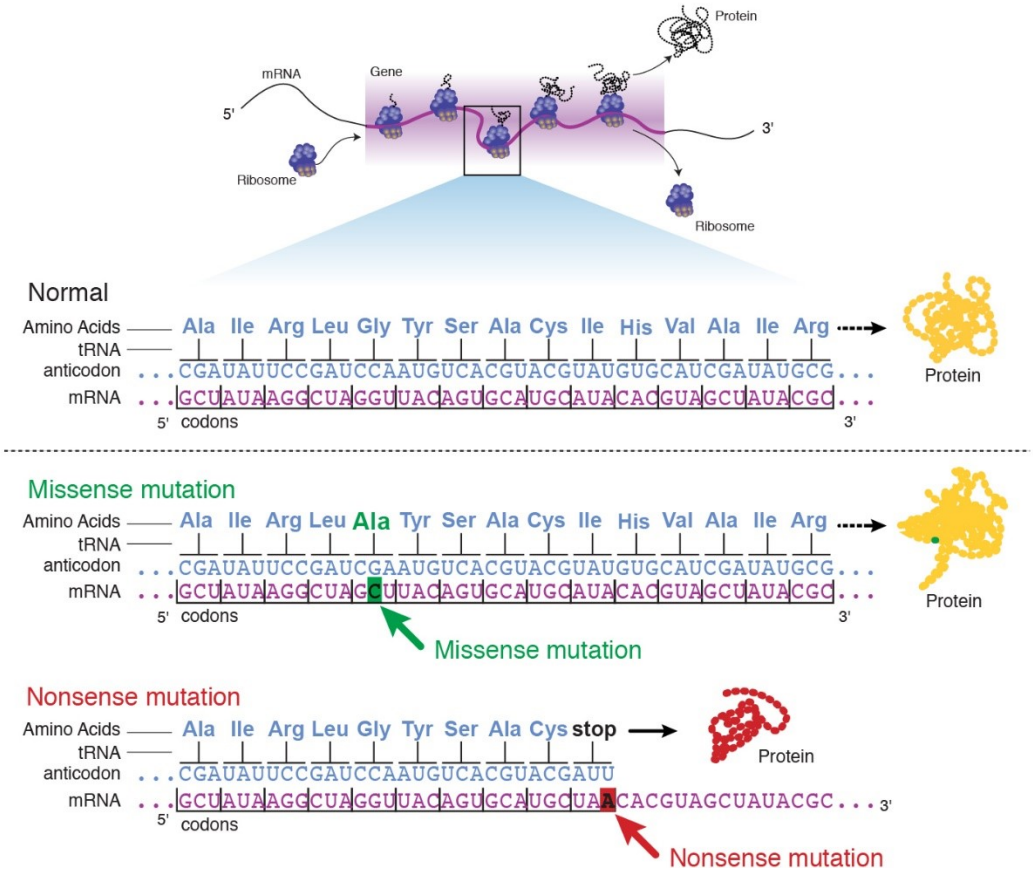

Figure 14: The effect of missense and nonsense mutations on protein synthesis(116).

1.11. Genetic Testing

In the last decade new technologies such as next generation sequencing (NGS) led to great improvements in genetic testing. The term NGS describes different technologies, which made it possible to quickly determine the DNA sequence of large amounts of DNA. These methods allow us to sequence the entire human DNA (genome) within weeks, while older methods took years for the same task. This great progress has made genetic testing more time- and cost-effective and therefore more available in clinical practice(117,118).

There exist several methods to analyse DNA and identify disease-associated variations. This chapter focuses on three, NGS based tests: whole-genome, whole-exome and targeted sequencing(117,118).

Whole-genome sequencing is the genetic analysis of the entire human genome including non-coding DNA. Even though non-coding DNA doesn't code for any proteins, it still has multiple functions in our bodies and alterations in these regions may affect gene activity and protein production. While for variants outside of the coding regions it is possible to cause genetic disorders, it is often not possible to tell whether a variant in the non-coding DNA is pathogenic or not. Therefore, it is hard to tell if such a variant is causal for a disease(117,118).

The human genome mainly consists of non-coding DNA, but as mentioned above, alterations in these regions are often hard to interpret. Exons instead make up only 1- 2 % of our DNA, yet they contain most of the currently identified, disease-causing mutations(118). Since most known pathogenic variants occur in coding regions, an efficient alternative method to whole-genome sequencing is whole-exome sequencing, which analyses only the coding DNA regions(117).

Targeted sequencing instead offers a more specific approach of DNA sequencing. In contrast to whole-genome and whole exome sequencing, this method makes it possible to analyse selected regions of interest. It allows targeted testing of specific exons, genes or even group a of genes, which are linked to the genetic disorder of interest. Of course, this approach is best used for genetic disorders, where the majority of candidate genes is already known. This method is useful for clinical diagnostics, since the genes chosen for this approach can be reliably assigned to a phenotype(119).

NGS has massively improved genetic testing. Modern tests can identify many disease-associated alterations in the human genome(118). Yet one of the limitations of NGS genetic testing is variant interpretation. For a lot of variants there is still limited information about their pathogenicity. It's often not possible to predict the severity of a genetic disorder or the rate of disease progression(120).

1.12. Genetic Subtypes

USH is a genetically heterogeneous disease. In total 16 loci (see Table 2) have been linked to the disorder and 13 causal genes have been identified. Of the 13 known USH genes, six lead to USH type 1, four to type 2 and three are associated with type 3. USH genes code for different proteins and current knowledge suggests, that these proteins interact in complex protein networks. These protein complexes are located in the inner ear, where they contribute to the differentiation and maintenance of inner ear hair bundles, and in the retina, where USH proteins are found in photoreceptors, in retinal pigment epithelium (RPE) and in synaptic terminals. The function of USH proteins in the retina is less clear than in the inner ear, because animal models often do not express a retinal phenotype(40).

This chapter discusses the different genetic subtypes, their causal genes (if known) and their gene products. Table 1 provides an overview of the genetic subtypes, which occur in Europe according to Bonnet et al. 2016(3).

Prevalence by clinical USH type	Prevalence by genetic subtype
USH type 1 (36%)	Type 1B (69.5%)
	Type 1C (7.1%)
	Type 1D (13%)
	Type 1F (7.8%)
	Type 1G (2.6%)
USH type 2 (60.4%)	Type 2A (91.5%)
	Type 2C (8.5%)
USH type 3 (2.1%)	Type 3A (100%)

Table 1: Prevalence of the genetic subtypes in Europe according to Bonnet et al. 2016(4).

Clinical type	Genetic subtype	Gene/ Locus	Inheritance	Protein	Protein Function
Reference (40)	Reference (121)	Reference (121)	Reference (121)	Reference (40)	Reference (40)
1	~~Type 1 A~~	Withdrawn[7]			
	Type 1 B	*MYO7A*	AR[8]	Myosin VIIa	Motor protein
	Type 1 C	*USH1C*	AR	Harmonin	Scaffold protein
	Type 1 D	*CDH23*	AR	Cadherin-23	Cell adhesion
	Type 1 E	*USH1E*	AR	*X*	*X*
	Type 1 F	*PCDH15*	AR	Protocadherin-15	Cell adhesion
	Type 1D/F	*CDH23 and PCDH15*	Digenic Recessive	Cadherins	Cell adhesion
	Type 1 G	*SANS*	AR	SANS	Scaffold protein
	Type 1 H	*USH1H*	*X*	*X*	*X*
	Type 1 J	*CIB2*	AR	CIB 2	Calcium and integrin binding
	Type 1 K	*USH1K*	AR	*X*	*X*
2	Type 2 A	*USH2A*	AR	Usherin	Cell adhesion
	Modifier of type 2 A	*PDZD7*	AR	PDZD7	Scaffold protein
	Type 2 C	*ADGRV1*	AR	VLGR1[9]	G-protein coupled receptor (GPCR)
		ADGRV1 and PDZD7	Digenic Recessive	VLGR1 and PDZD7	GPCR and Scaffold protein
	Type 2 D	*WHRN*	AR	Whirlin	Scaffold protein
3	Type 3 A	*CLRN1*	AR	Clarin-1	Subunit of ion channels?
	Type 3 B	*HARS*	AR	HARS	Histidyl-tRNA Synthetase

Table 2: Overview of the genetic USH subtypes, their causal genes/ genetic loci, their inheritance patterns and their encoded proteins (if known) as well as their function.

[7] See Gerber et al.(126)

[8] Autosomal Recessive

[9] Very large G protein-coupled receptor-1

1.13. Usher Type 1

USH1 genes code for proteins of different classes, which can be found in various body tissues. Studies have co-localized all USH1-proteins (except CIB2) in specific regions in retinal and inner ear hair cells. This common occurrence indicates, that they interact in a protein network there(102). CIB2 is the most recently detected USH1-protein, currently, only interactions with myosin VIIa and whirlin (USH2) have been documented(122). This chapter provides an overview of the USH1-genes and their gene products, except for USH type 1E (OMIM % 602097), USH type 1H (OMIM % 612632) and USH type 1K (OMIM % 614990). These genetic subtypes were only identified in a very small number of individuals. There exist only a few isolated cases and little is known about these subtypes(123–125). Since so little is known, they won't be discussed in this thesis.

1.13.1. Usher Type 1A

As illustrated in table 2 there exists no USH type 1A, which may be confusing at first. The reason for this irregularity can be explained historically.

USH type 1A has first been described in the early 90s, when the USH1A gene locus was mapped to the chromosome 14. The gene locus was known as the "French variety", because the USH1A locus has been reported in nine families originating from a small town in France. In the following years several candidate genes for the USH1A locus were investigated to find the causal genes for USH type 1A. The candidate genes were all sequenced in one individual from one of the nine families, but no disease-causing mutations were found. Further genetic examinations of the nine families surprisingly showed that seven of the nine families had mutations in the *MYO7A* gene, another family showed an association with USH1D and USH1E and one family was negative for all USH1 loci including the USH1A locus. Those results lead to the conclusion that there were no disease-associated alterations in connection to the USH1A locus and that in fact the USH1A locus does not exist(126).

1.13.2. Usher Type 1B

Mutations in *MYO7A* lead to USH type 1B and are the most common cause for USH type 1, accounting for ~69.5% of all cases in Europe(3). *MYO7A* encodes for an unconventional myosin, which is an actin-based motor protein with various functions in the retinal and inner ear cell and that is required for normal vision and hearing.

Analyses of mammalian animal models have shown that in the retina myosin VIIa is mostly expressed in RPE and in smaller amounts in photoreceptor cells. In the photoreceptor cells myosin VIIa is only present in the region of the connecting cilium, more specifically in the ciliary and periciliary membrane(127).

Studies suggest that myosin VIIa is involved in organelle transport, since it's required for correct melanosome localization and phagosome transport in the RPE. It's localization in the ciliary region of photoreceptors indicates involvement in protein transport along the connecting cilium. This hypothesis is supported by the accumulation of opsin, a protein involved in the visual cycle, in the ciliary region of test animals lacking functioning myosin VIIa. Myosin VIIa has multiple functions in the retinal cell, it's lack or malfunction leads to a series of cellular defects in the retinal cells. It is assumed that the combination of those defects leads to the retinal degeneration(127,128).

1.13.3. Usher Type 1C and Usher Type 1G

USH1C and *SANS* (Type 1G) both encode for scaffold proteins(102). This group of proteins can interact with multiple other proteins at the same time and organize them into an efficient protein complex(129).

USH1-proteins create this protein network by binding through protein-protein interaction domains, especially through the PDZ-domain of the protein harmonin(102). Simply put, a PDZ-domain is a part of a protein, that can interact with other proteins(130). In the inner ear these protein networks are essential for hair cell differentiation. During hair bundle development, harmonin, cadherin-23 and myosin VIIa form a functional network, which is essential for the cohesion of hair bundles. In test animals defects in these networks lead to hair bundle disorganisation, which consecutively led to congenital deafness(131).

USH1-protein networks are also found in synaptic terminals of photoreceptor cells and cochlear hair cells, which suggests their involvement in mechanosensitive transduction in the inner ear. In photoreceptors the defective USH1-complexes may lead to synaptic dysfunction resulting in RP(102,132).

1.13.4. Usher Type 1D and Usher Type 1F

USH type 1D and 1F are caused by mutations in *CDH23* and *PCDH15*. Both genes encode for cadherins, which are proteins responsible for cell-cell adhesion. *CDH23* codes for Cadherin-23 and *PCDH15* for Protocadherin-15(4).

CDH 23 and PCDH 15 are not only part of the USH1-protein network, but they also interact with each other. Together they form the tip links of the stereocilia's in the inner ear. Tip links are essential for mechanoelectrical transduction, and therefore important for hearing and movement(133).

1.13.5. Usher Type 1J

CIB2 encodes the calcium- and integrin-binding protein 2. Mutations in CIB2 either lead to non-syndromic hearing loss or USH type 1J, one of the rarer USH1 types. The protein can be found in the inner ear and in the retina, but is also expressed in skeletal muscle and brain tissue(122).

In the retina CIB2 is present in photoreceptors and RPE and in the inner ear it is found in hair cells and their stereocilia, which might indicate that CIB2 is involved in the mechanoelectrical transduction in the inner ear. Current data also suggests that CIB2 interacts with two other USH proteins, myosin VIIa and whirlin, but the mechanisms of this interaction have not been discovered yet. The same goes for the full biological function of CIB2 and the pathways leading to USH 1J, which largely remain unclear(134).

1.14. Usher Type 2

USH type 2 is the most common clinical USH type, with a prevalence of ~60% in Europe. Up to date four causal genes (*USH2A, ADGRV1, WHRN and PDZD7*) have been identified for USH type 2(3). Like the USH1-genes, the four USH2-genes encode for different proteins, which are also found in the retina and inner ear. USH2-proteins form a functional unit and are also known to interact with USH1-proteins(4). The fact, that both protein groups are incorporated into a mutual network, might indicate a common pathophysiological pathway for the different USH types. If one protein in this complex is lacking or non-functional, this one defect protein might disrupt the whole network, which ultimately ends in sensorineural degeneration(102).

1.14.1. Usher Type 2A and Usher Type 2C

USH type 2A is caused by mutations in the identically named gene (*USH2A*). It's one of the most common genetic USH subtypes and accounts for up to ~91.5% of all USH type 2 cases in Europe(3). Less frequent, mutations in *USH2A* cause atypical USH and non-syndromic RP(135).

USH2A encodes a protein called usherin, which has been localized in the region of the connection cilium of photoreceptors and in the inner ear's hair cells. Its exact position in the retina seems to be the inner segments membrane, which wraps around the connecting cilium. In the retina usherin contributes to the long-term maintenance of photoreceptors. This theory is based on the fact, that usherin-null mice develop a morphologically normal, well-functioning retina during their first months of life, but with increasing age they start to show signs of retinal degeneration. At 20 months old they have already lost over 50% of their photoreceptors. These findings as well as the slow progression of RP in USH suggest that usherin plays a vital role in long-term preservation of photoreceptors and the retina(136).

As mentioned above usherin is also located in the ear, where it has been co-localized with the protein VLGR1b[10] at the base of developing stereocilia of inner ear hair cells. VLGR1b is encoded by the gene *ADGRV1*, which is the causal gene for USH type 2C. The two proteins form transient links between adjacent stereocilia, called ankle links, which are important for correct hair bundle development and, when absent, result in deafness(137).

1.14.2. Usher Type 2D

USH type 2D is caused by mutations in the gene *WHRN*, which encodes the protein whirlin, a PDZ-domain containing scaffold protein. Mutations in *WHRN* are rare, with a prevalence of 0-9,5% in Europe and are also known to cause non-syndromic deafness(3,138).

Whirlin is expressed in photoreceptor cells, where it has been colocalized with the other two USH2-proteins usherin and VLGR1 in the periciliary membrane region[11]. The three proteins are thought to interact in a functional unit, and it seems that their expression is co-dependent, since photoreceptors which were missing whirlin also showed decreased levels of usherin and VLGR1. Furthermore, the loss of whirlin led to the misplacement of the other two proteins within the photoreceptors(138).

Photoreceptors of whirlin-knockout mice eventually underwent apoptosis and the laboratory mice started to show signs of retinal degeneration in their second year of

[10] Very large G protein-coupled receptor 1

[11] The periciliary membrane, is a membrane surrounding the connecting cilium.

life(139). These findings indicate that whirlin is important for the assembly of the USH2-protein network and that dysfunctions in this network are the primary cause for retinal degeneration(138,139).

But whirlin does not only interact with USH2-proteins, it has also been proven to interact with USH1-proteins. It takes part in the USH-protein complex, forming the central core together with harmonin and SANS(4).

1.14.3. PDZD7-associated phenotypes

The gene *PDZD7* encodes the PDZ domain-containing protein 7, a protein found in the ciliary region of photoreceptors, RPE and inner ear. The *PDZD7* gene product is integrated in the USH2-protein network, which is located at the periciliary membrane complex in photoreceptors and at the ankle link region in developing inner ear hair cells. Protein defects in the inner ear network lead to disorganisation of the developing stereocilia and consecutively to hearing loss(140), while in photoreceptors defects might disrupt protein trafficking at the ciliary region. This network dysfunction in the cilium probably inhibits protein transport from inner to outer segment(106).

PDZD7 is associated with two USH subtypes and is a causal gene for recessive, non-syndromic hearing loss. Mutations in *PDZD7* were found in combination with mutations in *USH2A* (USH type 2A) and *ADGRV1* (USH type 2C). In patients with mutations in *PDZD7* and *USH2A*, *PDZD7* works as a modifier gene for retinal disease expression. As a modifier gene *PDZD7* influences the retinal disease severity, which helps explain the phenotypic variability of USH. Patients with mutations in both, *USH2A* and *PDZD7*, might express a more severe visual phenotype than patients with mutations only in *USH2A*(106,141).

As mentioned above *PDZD7* is also associated with USH type 2C. Mutations in *PDZD7* and *ADGRV1* are known to cause digenic USH type 2C. Although digenic inheritance seems to be rare among USH patients, this proves that USH is not a disorder strictly inherited by mendelian laws(106).

1.15. Usher Type 3

USH type 3 is the rarest clinical type, with a worldwide prevalence of 3%. Yet, in some isolated populations[12] USH type 3 accounts for ~40% of all USH cases(3).

[12] High prevalence in Finland and among Ashkenazi Jews

To date three genes are associated with USH type 3, *CLRN1* (USH type 3A) and *HARS* (USH type 3B)(142) and *ABDH12*[13]. The gene *CLRN1* encodes clarin-1, a transmembrane protein of unknown function, which is found in the inner ear and retina. In the inner ear clarin-1 is expressed in hair cells and in the afferent neurons, that innervate them. There have been varying reports about clarin-1 expression in retinal cells, but several research groups have localized the protein in photoreceptors. Clarin-1 has been mainly found in the inner segment, connecting cilium and outer plexiform layer, a distribution similar to the other USH proteins, suggesting its involvement in the usher complex(143,144). In fact, an interaction between the tip link forming PCDH15 (USH type 1F) and Clarin-1 has been proven in test animals(145).

While the specific function of clarin-1 remains unknown, pathologic changes in *CLRN1* mutated mice suggest, that clarin-1 takes part in hair bundle development and maintenance as well as synapse maturation in the inner ear. Yet its role in retinal cells remains unknown(145).

Even less is known about USH type 3B, which is caused by mutations in the causal gene *HARS*. The gene *HARS* encodes histidyl-tRNA synthetase, which is a protein involved in protein synthesis. Mutations in *HARS* cause RP, progressive hearing impairment as well as episodic psychosis, which is not a typical USH symptom(40).

1.16. Atypical Usher

USH patients are clinically classified according to their ocular, auditory and vestibular symptoms. Although not all patients fit into these three clinical USH types, this historic classification remains in clinical use. Patients whose symptoms are non-consistent with the traditional classification are classified as atypical USH(1).

Atypical USH is also caused by mutations in the USH genes, which often have a wide phenotypic spectrum. For instance, mutations in *MYO7A* can lead to USH type 1, atypical USH and non-syndromic dominant or recessive deafness(1). While hearing loss in USH type 1 patients is non-progressive, patients with atypical USH, caused by mutations in *MYO7A*, can suffer from progressive hearing loss(146).

[13] USH associated mutations in the gene ABDH12 have only been identified in a few non-Caucasian families(5).

Another gene associated with atypical USH is *USH1G*. Usually mutations in this gene lead to an USH type 1 phenotype, characterized by congenital hearing loss, early onset RP and vestibular dysfunction. Yet, mutations in *USH1G* can also cause atypical USH, with moderate to severe HL, mild RP and normal vestibular function, a phenotype more typical for USH type 2. This diversity in gene expression emphasises the difficulty of predicting a clinical phenotype and individual prognosis(147). Aside from mutations in *MYO7A* (USH type 1B) and *USH1G* following genes have been associated with atypical USH: *CDH23* (USH type 1D) and *USH2A*(148).[14]

[14] In addition to the known USH genes, recently another gene has been associated with atypical USH: *CEP250* (Centrosomal protein 250). *CEP250* encodes a protein involved in centrosome cohesion during the cell cycle(7).

2. Methods

This study was carried out by the Department of Ophthalmology of the Medical University of Graz in collaboration with the Institute of Human Genetics of the Medical University of Graz and the Institut de la Vision of the Sorbonne Université (Paris, France).

2.1. Study Design and Trial Objectives

"The mutational landscape of patients with Usher syndrome in southern Austria" is a prospective cross-sectional, single-centre study. The primary objective of this study was to estimate the prevalence of the *USH2A*:c.11864G>A (p.Trp3955*) variant in southern Austria. Our hypothesis is that the prevalence of the mutation in the *USH2A* gene is higher than 8% in our patient population. Furthermore, we wanted to identify the disease-causing mutations among our USH patients.

2.2. Patient Recruitment

We searched the patient records of the Department of Ophthalmology of the University Hospital Graz for suitable USH patients. They were recruited and examined between January 2018 until July 2018.

2.3. Inclusion and Exclusion Criteria

To be eligible for study enrolment, patients had to have clinically confirmed USH. Patients, who during the ophthalmologic examination showed indications that their symptoms were not caused by USH or patients unable to give consent were excluded from our study.

2.4. Patient Number

Our primary endpoint is the prevalence of the W3955X mutation in USH patients in southern Austria. To estimate the prevalence of the mutation, we calculated a required sample size of n=20. Based on clinical data, a proportion of 8% in the study population is assumed.

The following formula was considered for the sample size estimation:

$$n \geq \left(\frac{z}{m}\right)^2 \times \hat{p}(1-\hat{p})$$

- n is the required sample size
- z is the Z-score (i.e. the boundary for the area of $\frac{\alpha}{2}$ in the standard normal distribution): 1.96 by normal approximation to the binomial distribution
- m is the desired margin of error: 12%
- $\hat{p}$ is the mutation prevalence in the overall study population: 0.08

2.5. Study Population

In total we included 17 USH patients in our study, ten female and seven male subjects from the following Austrian regions: Styria, Burgenland and Carinthia. We had no age limits for study enrolment and ages among patients ranged from 18 to 83 years with a mean of 48 years and a standard deviation of 17 years. Out of the 17 subjects only two had already undergone genetic testing. To our knowledge no subjects are related to each other or consanguineous.

2.6. Ophthalmologic Examination

Prior to genetic testing our patients underwent six ophthalmologic examinations, to verify the clinical diagnosis USH and to assess the current disease stage. A description of the examinations can be found in the chapter 3.2.4. Following ophthalmologic examinations, where performed on our patients:

- Best-corrected Visual Acuity
- Fundus Examination by Slit Lamp Examination
- Goldmann Perimetry
- Optical Coherence Tomography
- Full-field Electroretinogram
- Fundus Autofluorescence

2.7. Genetic Analysis

After the ophthalmologic examination and the confirmation of the clinical diagnosis USH, blood samples of our patients were collected and sent to the Institute de la Vision, Paris, France. Due to its high genetic heterogeneity, it is difficult to reliably diagnose USH, therefore different techniques were applied to identify DNA sequence variants and copy number variations. After isolating DNA from the peripheral blood samples with standard methods, targeted exome sequencing was

performed. All coding and non-coding exons of ten USH associated genes were analysed. If no mutation or only a monoallelic mutation was found by targeted exome sequencing a SNP array analysis was performed, to identify copy number variations.

3. Results

3.1. Patients

A total of 17 USH patients were included in the study – ten female and seven male patients. Their ages ranged from 18 to 83 years with an average age of 48 years (SD 17). The age and gender distribution is shown in Table 3 and Table 4. No patients were excluded or withdrew after enrolment.

Gender	Number of patients	Percentage	Valid percent
Male	7	41.2	41.2
Female	10	58.8	58.8
Total	17	100.0	100.0

Table 3: Gender distribution

	Age
N valid	17
N missing	0
Mean value	48.059
Standard deviation	16.626
Minimum	18
Maximum	83

Table 4: Age distribution

3.2. Ophthalmologic Results

3.2.1. Best-corrected Visual Acuity

The best corrected visual acuity (BCVA) was documented as decimal acuity. The results have been converted to a LogMAR scale for statistical analyses. The following formula has been used for the conversion: logMAR = -log (decimal acuity)(149).

Two out of 17 USH patients had such a poor visual acuity that they were not able to take a standardized visual acuity test using an eye chart. Their visual acuity was assessed by using the semiquantitative scale “counting fingers” at the distance of

one meter. The BCVA of the two subjects was estimated at a decimal acuity of 0.02(150). The estimated measurement of 0.02 was used for statistical analyses.
According to the ICD-10 criteria for low vision (only taking into account the best corrected visual acuity and not the visual field) out of the 17 patients two were blind, one patient had a severe vision impairment, one patient had a moderate to severe vision impairment and one patient a moderate vision impairment. Twelve patients had a mild or no vision impairment(151).
The mean visual acuity (LogMAR) of all subjects was 0.49 (SD 0.5) on the right eye and 0.57 (SD 0.5) on the left eye. The results ranged from 1.7 to -0.1. The values are listed in Table 5.

	Best corrected visual acuity – LogMAR	
	Right eye	Left eye
N valid	17	17
N missing	0	0
Mean value	0.494	0.570
Standard deviation	0.510	0.530
Minimum	-0.0969	0.0969
Maximum	1.699	1.699

Table 5: Best corrected visual acuity (LogMAR)

3.2.2. Visual Field Testing

The visual field testing was performed using Goldmann perimetry. We assessed the vertical and the horizontal field range of the right and the left eye. We defined our lower limit for the visual field testing as 5°. The examination could not be performed on three patients.
Six out of 14 patients had a very limited visual field with a remaining vertical and horizontal field range of 5° in both eyes. Additionally, two patients had a vertical and horizontal field range of 5° in one eye and a visual field of the better eye no greater than 10° in radius. Therefore, eight out of the 14 patients are considered blind according to the ICD-10 criteria for visual impairment(151).
The mean horizontal field range for the right eye was 26.1° (SD 36) and for the left eye 28.6° (SD 39). The mean vertical field range was 20.7° (SD 27) for the right eye

and 21.1° (SD 27) for the left eye. The results ranged from 5° to 120° horizontally and 5° to 95° vertically. The values are listed in table 6.

	Goldmann horizontal		Goldmann vertical	
	Right eye	Left eye	Right eye	Left eye
N valid	14	14	14	14
N missing	3	3	3	3
Mean value	26.071	28.571	20.714	21.0714
Standard deviation	35.636	39.293	27.165	26.903
Minimum	5	5	5	5
Maximum	120	120	95	80

Table 6: Visual field testing - Goldmann perimetry

3.2.3. Electroretinogram

Electroretinograms (ERG) could not be performed on all patients. On those patients willing to undergo an ERG exam, one was performed during the clinical study. Otherwise, if a patient had already undergone an ERG exam in the past, the results of these exams were used.

In total we acquired ERGs of seven USH patients, which were performed between 2001 and 2018. The rod-, combined- and flicker-responses were measured.

All subjects had reduced ERG responses at the time of measurement. Four patients even had extinguished ERG responses.

	ERG rods [µV]		ERG combined [µV]		ERG Flicker [µV]	
	Right	Left	Right	Left	Right	Left
N valid	7	7	7	7	7	7
N missing	10	10	10	10	10	10
Mean value	8.469	7.753	14.257	4.819	11.497	2.070
Standard deviation	13.190	12.283	20.103	9.998	18.137	2.712
Minimum	0.00	0.00	0.00	0.00	0.00	0.00
maximum	31.80	29.90	51.90	26.70	46.60	6.34

Table 7: ERG measurements (µV)

3.2.4. Optical Coherence Tomography

Using an OCT scan, we measured the subfoveal retinal thickness, the choroidal thickness and the retinal nerve fiber layer (RNFL) thickness. The retinal thickness and the RNFL were calculated automatically by an OCT mapping software, while the choroidal thickness was measured manually.

The subfoveal retinal thickness was measured in all subjects (n=17). We assume a normal value of 250 µm for the subfoveal retinal thickness. In our subjects the mean subfoveal retinal thickness was 237 µm (SD 47) for the right eye and 237 µm (SD 50) for the left eye. The subfoveal retinal thickness ranged from 151 µm to 327 µm. The values are shown in table 8.

The choroidal thickness was assessed in 15 patients. We assume 250 to 350 µm to be a normal thickness of the subfoveal choroid(152). In our subjects the mean choroidal thickness was 228 (SD 78) µm in the right eye and 231 µm (SD 87) in the left eye. The choroidal thickness ranged from 84 µm to 411 µm. The exact values are shown in table 8.

	Retinal thickness [µm]		Choroidal thickness [µm]	
	Right eye	Left eye	Right eye	Left eye
N valid	16	16	15	15
N missing	1	1	2	2
Mean value	237.438	237.125	228.4	231.133
Standard deviation	46.600	49.680	77.857	87.191
Minimum	155	151	91	84
Maximum	310	327	369	411

Table 8: Subfoveal retinal thickness and choroidal thickness (µm)

The RNFL thickness was measured in 7 patients. The mean RNFL thickness was 119 microns (SD 14) for the right eye and 119 microns (SD 15) for the left eye. The RNFL thickness ranged from 104 to 150 microns. The exact values are shown in table 9.

	Retinal nerve fibre layer [µm]	
	Right eye	Left eye
N valid	7	7
N missing	10	10
Mean value	119.143	119
Standard deviation	14.029	14.663
Minimum	104	106
Maximum	143	150

Table 9: Retinal nerve fibre layer thickness (µm)

In our seven subjects two patients had a normal RNFL thickness and five patients had an increased RNFL thickness. No subject had a loss in RNFL thickness. The normal values used for the evaluation of the RNFL thickness are age-dependent and machine-specific values.

		RNFL right eye			RNFL left eye		
		number	percentage	valid percentage	number	percentage	valid percentage
N valid	Normal	2	11.765	28.571	2	11.765	28.571
	too thick	5	29.412	71.429	5	29.412	71.429
	all	7	41.176	100.000	7	41.176	100.000
N missing		10	58.824		10	58.824	
N total		17	100.000		17	100.000	

Table 10: Evaluation of the RNFL thickness (µm)

3.2.5. Distribution of Measurements

The following Q-Q plots show the distribution of the measured values of best-corrected visual acuity, subfoveal retinal thickness and subfoveal choroidal thickness compared to a normal distribution. These plots show that the measured values are close to a theoretical gaussian distribution for all three measurements.

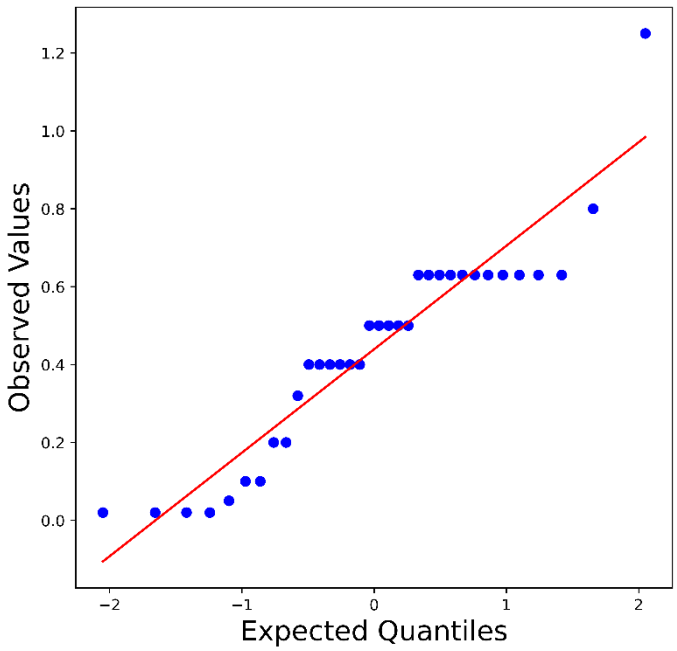

Table 11: Q-Q Plot of Best Corrected Visual Acuity (decimal acuity)

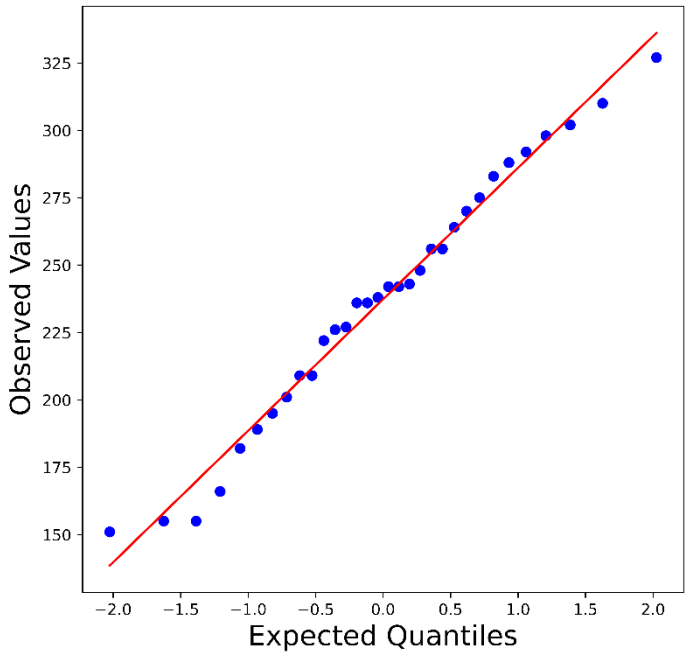

Table 12: Q-Q Plot of Subfoveal Retinal Thickness (µm)

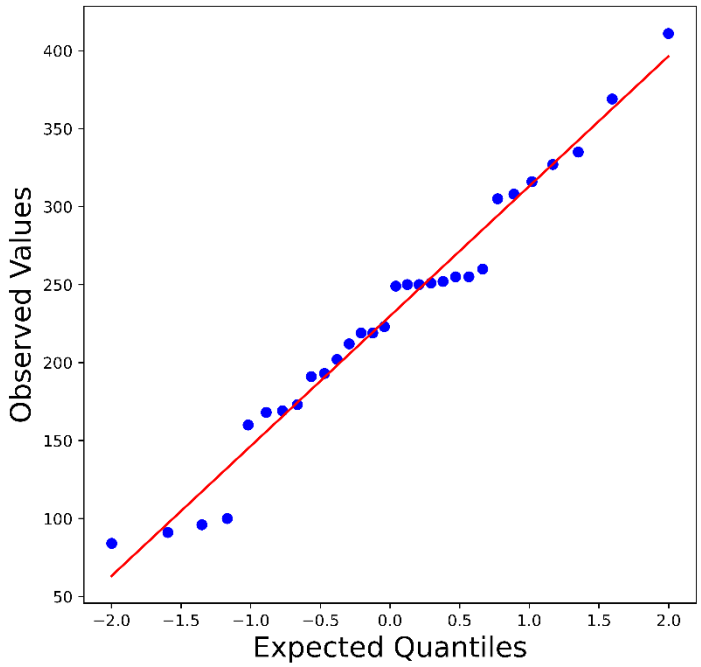

Table 13: Q-Q plot of Subfoveal Choroidal Thickness (µm)

3.2.6. Correlation of Visual Acuity and Retinal Thickness

The BCVA of the left and the right eye correlated significantly (p=0.05) as shown in table 14 and 15. This was expected since USH affects both eyes. In our subject population both eyes were approximately equally affected.

The left BCVA and the left retinal thickness correlated, but not significantly (p=0.119) as shown in table 14. This might be due to our limited number of USH patients. The right BCVA and the right retinal thickness correlated significantly (p=0.05) as seen in table 15. This correlation between retinal thickness in OCT scans and visual function was expected. The retinal thickness of the left and right eye correlated significantly, which highlights the bilateral symmetry of typical RP.

		BCVA right	Retinal thickness left
BCVA left	Korrelation (pearson)	0.682	0.405
	Significance (2 sided)	0.00358	0.119
	N	16	16

Table 14: Correlation of the left BCVA (decimal) and the left retinal thickness (µm)

		BCVA left	Retinal thickness right
BCVA right	Korrelation (pearson)	0.682	0.581
	Significance (2 sided)	0.00358	0.0183
	N	16	16

Table 15: Correlation of the right BCVA (decimal) and the right retinal thickness (µm)

3.2.7. Correlation of Visual Acuity and Choroidal Thickness

We evaluated if there was a correlation between the BCVA and the choroidal thickness. In our study population there was no significant correlation between BCVA and choroidal thickness as shown in Table 16 and 17.

		Left choroidal thickness
Left BCVA	Korrelation (pearson)	-0.161
	Significance (2 sided)	0.567
	N	15

Table 16: Correlation between BCVA and choroidal thickness (µm) of the left eye

		Right choroidal thickness
Right BCVA	Korrelation (pearson)	-0.201
	Significance (2 sided)	0.473
	N	15

Table 17: Correlation between BCVA and choroidal thickness (µm) of the right eye

3.2.8. Correlation of Visual Field and OCT Measurements

We checked for correlations of the visual field with the retinal thickness and the choroidal thickness. As shown in table 18 there is a significant correlation (p=0.05) between the horizontal and vertical visual field with the retinal thickness in both eyes. In contrast we were not able to show a significant correlation of the visual field with the choroidal thickness.

		Retinal thickness left	Retinal thickness right	Choroidal thickness left	Choroidal thickness right
Goldmann horizontal left	Correlation (spearman-rho)	0.777	0.702	0.172	0.209
	Significance (2 sided)	0.00108	0.00515	0.558	0.473
	N	14	14	14	14
Goldmann horizontal right	Correlation (spearman-rho)	0.712	0.625	0.221	0.271
	Significance (2 sided)	0.00428	0.0168	0.447	0.350
	N	14	14	14	14
Goldmann vertical left	Correlation (spearman-rho)	0.788	0.689	0.156	0.191
	Significance (2 sided)	0.0008113	0.00638	0.596	0.514
	N	14	14	14	14
Goldmann vertical right	Correlation (spearman-rho)	0.814	0.731	0.203	0.261
	Significance (2 sided)	0.000395	0.00297	0.487	0.367
	N	14	14	14	14

Table 18: Correlation of Visual Field and OCT measurements

3.2.9. Correlation of Age and Ophthalmologic Results

Our results show that there is a significant negative correlation ($p \leq 0.05$) of a patient's age with the visual field as shown in table 19.

		Goldmann horizontal left	Goldmann horizontal right	Goldmann vertical left	Goldmann vertical right
Age	Correlation (spearman-rho)	-0.618	-0.560	-0.588	-0.634
	Significance (2 sided)	0.0185	0.0373	0.0271	0.0148
	N	14	14	14	14

Table 19: Correlation of Visual Field with a Patient's age

We were not able to show a significant correlation of a patient's age with the BCVA, the retinal thickness or the choroidal thickness as shown in table 20.

		BCVA left	BCVA right	Retinal thickness left	Retinal thickness right	Choroidal thickness left	Choroidal thickness right
Age	Correlation (pearson)	-0.0608	-0.369	-0.204	-0.245	-0.439	-0.454
	Significance (2 sided)	0.817	0.145	0.449	0.361	0.102	0.0891
	N	17	17	16	16	15	15

Table 20: Correlation of a Patient's Age with the Ophthalmologic Results

3.3. Genetic Results

Of the 17 subjects enlisted in the study, two had already undergone genetic testing. In these two patients their pre-existing results were used for this study. On the other 15 subjects genetic testing was performed by using targeted exome sequencing and SNP-array-analysis. In 73.34% (11/15) two mutations were identified in one of the USH genes. With the exception of one subject, which had a homozygous mutation, we assume that the detected mutations are biallelic (compound-heterozygous), since USH is an autosomal-recessive disease. However, no genetic testing was performed on the patient's parents. In 13.34% (2/15) monoallelic mutations were identified. In on patient (6.67%) no mutation was detected and in one patient (6.67%) a homozygous deletion of exon 20 in the *CDH23* gene was found, which should be further evaluated by using real-time PCR.

Including the pre-existing results of the two patients, which already underwent genetic testing, mutations were detected in 94.12% (16/17) of our study population. In 76.47% (13/17) of cases two mutations were identified, in 11.76% (2/17) monoallelic mutations were found and in one case (5.88%) a homozygous deletion of exon 20 on the gene *CDH23* was detected. In one case (5.88%) no mutation was detected through targeted exome sequencing and SNP-array-analysis.

88.24% (15/17) of the mutations were located in genes associated with USH type 2. Out of these the majority of mutations, namely 76.47% (13/17), were detected in the *USH2A* gene. Mutations in the USH type 2 associated gene *ADGRV1* were found in 11.76% (2/17). No mutations were detected in the remaining USH type 2 associated genes. One mutation was found in an USH type 1 associated gene. We

detected a homozygous deletion of exon 20 in the *CDH23* gene in one patient. This genetic alteration has to be further evaluated via real-time PCR. No variants were found in USH type 3 associated genes. The distribution of the affected USH genes is illustrated in table 21.

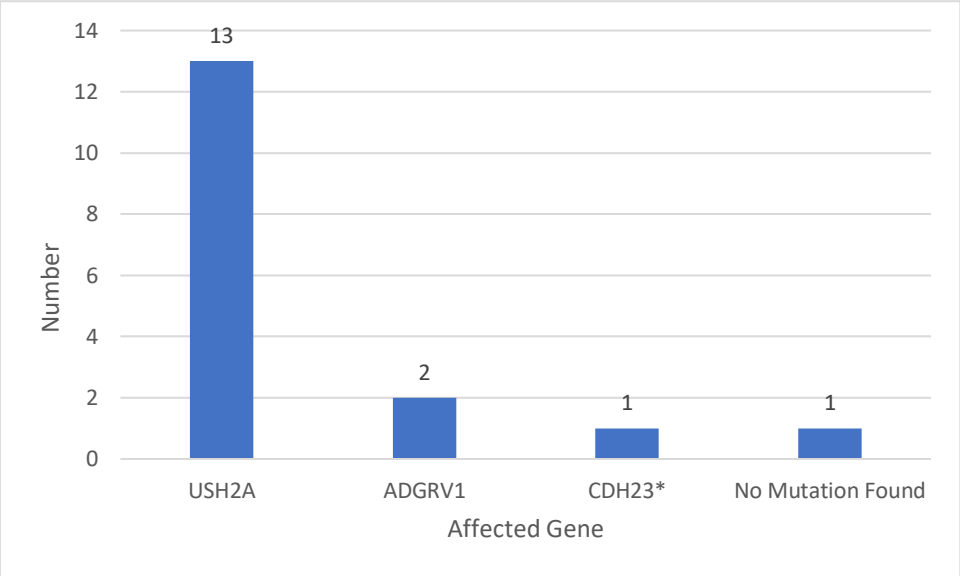

Table 21: Distribution of Affected Genes

(*the deletion on CDH23 needs to be further evaluated through real-time PCR)

In total we identified 17 allelic variants in our USH patients. We detected nonsense- (50%), frameshift- (21.43%), missense- (10.72%) and splice site mutations (17.86%). The most common mutation was *USH2A*:c.11864G>A (p.Trp3955*), which was found in five subjects. The second most common mutation was *USH2A*:c.6782G>A (p.Trp2261*), which was detected in four subjects. The table 22 shows the detected variants and their molecular consequence.

In our study population the most frequent mutation was *USH2A*:c.11864G>A (p.Trp3955*). We assumed a prevalence > 8% of this mutation in southern Austria based on the geographic proximity between Austria and Slovenia and the findings of Bonnet et al 2016(3). We found a monoallelic *USH2A*:c.11864G>A (p.Trp3955*) mutation in five subjects (29.41%), which was significantly higher than 8% (p=0.05).

Gene	Variant 1	Variant 2	Molecular Consequence		Interpretation	
			Variant 1	Variant 2	Variant 1	Variant 2
USH2A	c.6782G>A, p.Trp2261*	c.11864G>A, p.Trp3955*	nonsense	nonsense	likely pathogenic	pathogenic
USH2A	c.11864G>A, p.Trp3955*	No mutation detected	nonsense	/	pathogenic	/
USH2A	c.10042_10043dup, p.(Lys3349Leufs*9)	c.12234_12235del, p.(Asn4079Trpfs*19)	frameshift	frameshift	pathogenic	pathogenic
USH2A	c.6782G>A, p.Trp2261*	c.11499_11505del, p.(Leu3834Hisfs*7)	nonsense	frameshift	likely pathogenic	pathogenic
USH2A	c.1805G>A, p.Gly602Glu	c.11864G>A, p.Trp3955*	missense	nonsense	uncertain significance	pathogenic
USH2A	c.6782G>A, p.Trp2261*	c.5167+1G>A	nonsense	splice site	likely pathogenic	unclassified variant
USH2A	c.2209C>T, p.Arg737*	c.6657+3_6657+6del	nonsense	splice site	pathogenic	pathogenic
USH2A	c.920_923dup, p.(His308Glnfs*16)	c.2299del, p.(Glu767Serfs*21)	frameshift	frameshift	pathogenic	pathogenic
USH2A	c.11864G>A, p.Trp3955*	No mutation detected	nonsense	/	pathogenic	/
USH2A	c.680T>A, p.Ile227Asn	c.6782G>A, p.Trp2261*	missense	nonsense	pathogenic	likely pathogenic
USH2A	c.920_923dup, p.(His308Glnfs*16)	c.11864G>A, p.Trp3955*	frameshift	nonsense	pathogenic	pathogenic
USH2A	c.2209C>T	c.6657+3_6657+6del	nonsense	splice site	pathogenic	pathogenic
USH2A	c. 6399G>A; p.W2133X	c.12889T>C; p.S4297P	nonsense	missense	pathogenic	uncertain significance
ADGRV1	c.9623+1G>A	c.9623+1G>A	splice site	splice site	likely pathogenic	likely pathogenic
ADGRV1	c.461C>A, p.Ser154*	c.8197C>T, p.Arg2733*	nonsense	nonsense	likely pathogenic	likely pathogenic

Table 22: Mutations found in the USH associated genes, their molecular consequence and pathogenicity

Of the 17 detected variants 58.82% are assumed to be pathogenic mutations, 23.53% are likely pathogenic variants and 17.65% are unclassified variants (see Table 22). The pathogenicity of the variants was evaluated by using ClinVar(153), ACMG standards and guidelines(154) and if available molecular biological evaluations.

4. Discussion

This study aims to identify variants in USH associated genes and their prevalence in southern Austria. To our knowledge so far, no clinical study has assessed the prevalent mutations in USH patients from this Austrian region. A study by Bonnet et al.(3) which tested 427 USH patients from six European countries[15] including Slovenia identified mutations in 93% of cases. The two most frequent mutations found in their study were *USH2A*:c.2299delG (p.Glu767Serfs*21) and *USH2A*:c.11864G4A (p.Trp3955*). Although these were the most common mutations, their geographical distribution varied widely. The most common mutation in Slovenia was the c.11864G4A variant in the *USH2A* gene with a prevalence of 82.5%(3). Due to the geographical proximity, we expected a similar mutational landscape in southern Austria and Slovenia. Therefore, we assumed a prevalence of the c.11864G4A variant > 8% in southern Austria. We included 17 USH patients in our study and were able to detect mutations in 94.12% (16/17). In our study population the most frequent mutation was *USH2A*:c.11864G>A (p.Trp3955*). This variant was found on one allele in five subjects (29.4%), which is significantly higher than 8% (p=0.05). This findings support our hypothesis that the mutational landscape in southern Austria may be similar to the one in Slovenia. Even though we have a very limited number of patients our results reflect the findings of Bonnet et al. that there exist regionally restricted mutations(3).

As mentioned above – besides the c.11864G4A variant – the most common variant found by Bonnet et al. in Europe was *USH2A*:c.2299delG (p.Glu767Serfs*21). This *USH2A* variant was found in 32.7% of cases in Germany, while it was not detected in their Slovenian study population(3). In our study population we have only one individual carrying this *USH2A* variant. Since our study was limited to southern Austria, we propose that the distribution of this variant might be higher in the northern regions of Austria. This hypothesis could be supported by Millán et al., who described a decreasing frequency of the c.2299delG variant from Northern to Southern Europe(4).

[15] The six European countries were Slovenia, Germany, France, Italy, Spain and Denmark.

USH type 2 is reported to be the most common USH type in Europe. Currently we know four genes associated with USH type 2. Disease-causing variants in the *USH2A* gene are by far the most common cause of USH type 2 in Europe(4,155). Our results correlate with these findings from other studies. In our study population 15 patients are classified as USH type 2 and one is classified as USH type 1. In total we were able to detect mutations in USH genes in 94.12% of our USH patients. Out of these 93.75% (15/16) were detected in USH2 genes and only one subject carried a mutation in an USH1 gene. Of the mutations found in USH2 genes, 86.67% (13/15) were detected on the *USH2A* gene. By comparison, in the study carried out by Bonnet et al. around 60% of USH patients were classified as USH type 2 and in 91.5% of these USH type 2 cases mutations in *USH2A* have been detected(3).

In one case we were not able to identify a possibly associated variant in the ten tested USH genes by using targeted exome sequencing and SNP-array-analysis. This might be due to the genetic heterogeneity of USH. Especially novel variants might not be detected by genetic screenings, which focus on previously reported variants.

Our exploratory objectives were to investigate genotype-phenotype correlations, since USH is a clinically and genetically heterogenous disease. The relatively large spectrum of the disease progression of RP in USH makes it difficult to determine an individual prognosis for the patients(47,155). We were not able to explore these correlations. For one, we only included 17 subjects, which is far too small to make any conclusive statements. Further, the small sample size makes it very difficult to make statistically significant predictions on the underlying population. Furthermore, many of the USH patients were not included in regular check-ups and only limited information is known about their disease onset and RP progression.

RP causes a bilateral symmetrical retinal degeneration in patients with USH(50,75). This symmetry is also seen in our clinical findings. In our subjects the retinal thickness of the left and the right eye correlated significantly. The BCVA and the visual field of the right and left eye also showed a high degree of symmetry.

RP is a chronic disease, which leads to a progressive loss of photoreceptor cells. OCT scans of patients with RP show a reduced outer segment and outer nuclear

layer thickness. It has been previously reported that a decrease in retinal thickness has been associated with a decrease in visual functions, in particular with a loss in visual field sensitivity(57,156). This correlation between retinal thickness and visual field is also noticeable in our subjects. Visual field and retinal thickness had a positive correlation. However, we did not find a strong correlation between BCVA and retinal thickness on both eyes, which might be due to our low patient number.

A decrease in choroidal thickness in RP and USH in comparison to healthy eyes was described in previous studies(157,158). In our subjects the choroidal thickness was reduced in seven out of 15 patients, but we did not find a significant correlation between the choroidal thickness and visual function.

RP in USH is a progressive disease, therefore we expected a more limited visual function with increasing age. Indeed, we did find a significant correlation between age and visual field loss. In our study population the subjects with a severely reduced visual field were all over 40 years old. Although we were able to show a connection between a decrease in visual field and age, we did not find a significant correlation of age with BCVA, retinal or choroidal thickness.

The main limitation of our study was the low number of included patients. We were not able to include our goal of 20 subjects. Furthermore, it was not possible to perform the eye examinations on all subjects, e.g. because of their comorbidities, which made it even more difficult to make statistically sound predictions on such a low number of subjects. Another limiting factor was that many of the patients were not included in regular check-ups. This made it difficult to assess their disease onset and progression. Combined with the low number of subjects, this made it impossible to establish a genotype-phenotype correlation. Furthermore, it is important to mention that some patients in a late stage of USH were not able to travel to the clinic and could therefore not partake in the study. This might have led to a selection bias due to the exclusion of more severe USH cases in our study.

Future studies should include a larger sample size. To further investigate phenotype-genotype correlations, patients should be followed up more closely for a larger period of time.

In conclusion, there seems to exist a large regional heterogeneity in the mutational landscape of USH patients in Europe. The mutational landscape in southern Austria seems to be similar to the one in Slovenia.

5. References

1. Yan D, Liu XZ. Genetics and pathological mechanisms of Usher syndrome. J Hum Genet [Internet]. 2010 Jun 9 [cited 2018 Feb 26];55(6):327–35. Available from: http://www.nature.com/articles/jhg201029
2. Daiger SP, Sullivan LS, Bowne SJ. Genes and mutations causing retinitis pigmentosa. Clin Genet [Internet]. 2013 Aug 1 [cited 2018 Mar 8];84(2):132–41. Available from: http://doi.wiley.com/10.1111/cge.12203
3. Bonnet C, Riahi Z, Chantot-Bastaraud S, Smagghe L, Letexier M, Marcaillou C, et al. An innovative strategy for the molecular diagnosis of Usher syndrome identifies causal biallelic mutations in 93% of European patients. Eur J Hum Genet [Internet]. 2016 Dec 27 [cited 2018 Mar 9];24(12):1730–8. Available from: http://www.nature.com/articles/ejhg201699
4. Millán JM, Aller E, Jaijo T, Blanco-Kelly F, Gimenez-Pardo A, Ayuso C. An update on the genetics of usher syndrome. J Ophthalmol [Internet]. 2011 [cited 2018 Mar 2];2011:417217. Available from: http://www.ncbi.nlm.nih.gov/pubmed/21234346
5. Eandi CM, Dallorto L, Spinetta R, Micieli MP, Vanzetti M, Mariottini A, et al. Targeted next generation sequencing in Italian patients with Usher syndrome: phenotype-genotype correlations. Sci Rep [Internet]. 2017 Nov 15 [cited 2018 Apr 11];7(1):15681. Available from: http://www.ncbi.nlm.nih.gov/pubmed/29142287
6. Li T, Feng Y, Liu Y, He C, Liu J, Chen H, et al. A novel ABHD12 nonsense variant in Usher syndrome type 3 family with genotype-phenotype spectrum review. Gene. 2019 Jul 1;704:113-120 [Internet]. 2019 [cited 2020 Dec 6]. Available from: https://pubmed.ncbi.nlm.nih.gov/30974196/
7. Khateb S, Zelinger L, Mizrahi-Meissonnier L, Ayuso C, Koenekoop RK, Laxer U, et al. A homozygous nonsense CEP250 mutation combined with a heterozygous nonsense C2orf71 mutation is associated with atypical Usher syndrome. J Med Genet [Internet]. 2014 Jul 29 [cited 2018 Aug 1];51(7):460–9. Available from: http://www.ncbi.nlm.nih.gov/pubmed/24780881
8. Abad-Morales V, Navarro R, Burés-Jelstrup A, Pomares E. Identification of a novel homozygous ARSG mutation as the second cause of Usher syndrome type 4. Am J Ophthalmol Case Rep. 2020;19:100736. Published 2020 May 8 [Internet]. 2020 [cited 2020 Dec 6]. Available from: https://www.ncbi.nlm.nih.gov/pmc/articles/PMC7235610/
9. Fu Q, Xu M, Chen X, Sheng X, Yuan Z, Liu Y, et al. CEP78 is mutated in a distinct type of Usher syndrome. J Med Genet. 2017 Mar;54(3):190-195 [Internet]. 2017 [cited 2020 Dec 6]. Available from: https://pubmed.ncbi.nlm.nih.gov/27627988/
10. Ahmed Z, Jaworek T, Sarangdhar G, Al E. Inframe deletion of human ESPN is associated with deafness, vestibulopathy and vision impairment. Journal of Medical Genetics 2018; 55:479-488. [Internet]. 2018 [cited 2020 Dec 6]. Available from: https://jmg.bmj.com/content/55/7/479.long
11. Hamel C. Retinitis pigmentosa. Orphanet J Rare Dis [Internet]. 2006 Oct 11 [cited 2018 Feb 26];1(1):40. Available from: http://ojrd.biomedcentral.com/articles/10.1186/1750-1172-1-40
12. Kahle W, Frotscher M. Taschenatlas Anatomie in 3 Bänden, Band 3: Nervensystem und Sinnesorgane. 11th ed. Stuttgart: Georg Thieme Verlag; 2013. 345–358, 366–378 p.

13. Schünke M, Schulte Er, Schumacher U. Prometheus, Lernatlas der Anatomie, Kopf, Hals und Neuroanatomie. 3., überar. Stuttgart: Georg Thieme Verlag; 2012. 152–164 p.
14. Grehn F. Augenheilkunde, 31., überarbeitete Auflage. Springer-Verlag Berlin Heidelberg; 2012. 5–9, 265–267 p.
15. Silversmith E. File:Focus in an eye.svg (CC BY-SA 2.5) [Internet]. Wikimedia Commons. 2006 [cited 2019 Sep 11]. Available from: https://commons.wikimedia.org/wiki/File:Focus_in_an_eye.svg
16. Kolb H. Simple Anatomy of the Retina. 2005 May 1 [Updated 2012 Jan 31] [Internet]. Kolb H, Fernandez E, Nelson R, editors. Webvision: The Organization of the Retina and Visual System. Salt Lake City (UT): University of Utah Health Sciences Center; 1995-; [cited 2019 Sep 9]. Available from: https://www.ncbi.nlm.nih.gov/books/NBK11533/
17. Rehman I, Mahabadi N, Motlagh M, Ali T. Anatomy, Head and Neck, Eye Fovea. [Updated 2019 Jun 5]. In: StatPearls [Internet]. Treasure Island (FL): StatPearls Publishing; 2019 Jan-; [cited 2019 Sep 9]. Available from: https://www.ncbi.nlm.nih.gov/books/NBK482301/
18. Purves D, Augustine GJ, Fitzpatrick D, Katz LC, LaMantia A-S, McNamara JO, et al., editors. Neuroscience [Internet]. 2nd ed. Sunderland (MA): Sinauer Associates; 2001. Functional Specialization of the Rod and Cone Systems; [cited 2018 Aug 22]. Available from: https://www.ncbi.nlm.nih.gov/books/NBK10850/
19. Loughman J, Davison PA, Nolan JM, Akkali MC, Beatty S. Macular pigment and its contribution to visual performance and experience. J Optom [Internet]. 2010 Apr [cited 2019 Sep 9];3(2):74–90. Available from: https://linkinghub.elsevier.com/retrieve/pii/S188842961070011X
20. Jamarchn, Rhcastilhos. File:Schematic diagram of the human eye en.svg (CC BY-SA 3.0) [Internet]. Wikimedia Commons. 2007 [cited 2019 Sep 11]. Available from: https://commons.wikimedia.org/wiki/File:Schematic_diagram_of_the_human_eye_en.svg
21. Lüllmann-Rauch R. Taschenlehrbuch Histologie, 3., vollständig überarbeite Auflage. Stuttgart: Georg Thieme Verlag; 2009. 587–591 p.
22. Strauss O. The Retinal Pigment Epithelium [Internet]. Webvision: The Organization of the Retina and Visual System. University of Utah Health Sciences Center; 1995 [cited 2018 Aug 20]. Available from: http://www.ncbi.nlm.nih.gov/pubmed/21563333
23. Sparrow JR, Hicks D, Hamel CP. The retinal pigment epithelium in health and disease. Curr Mol Med [Internet]. 2010 Dec [cited 2019 Sep 9];10(9):802–23. Available from: http://www.ncbi.nlm.nih.gov/pubmed/21091424
24. Bonilha VL, Rayborn ME, Bhattacharya SK, Gu X, Crabb JS, Crabb JW, et al. The retinal pigment epithelium apical microvilli and retinal function. Adv Exp Med Biol [Internet]. 2006 [cited 2019 Sep 9];572:519–24. Available from: http://www.ncbi.nlm.nih.gov/pubmed/17249618
25. Purves D, Augustine GJ, Fitzpatrick D, Katz LC, LaMantia A-S, McNamara JO, et al., editors. Neuroscience [Internet]. 2nd ed. Sunderland (MA): Sinauer Associates; 2001. The Retina; [cited 2019 Sep 9]. Available from: https://www.ncbi.nlm.nih.gov/books/NBK10885/
26. Pradeep T, Waheed A. Histology, Eye. [Updated 2019 Jul 9]. In: StatPearls [Internet]. Treasure Island (FL): StatPearls Publishing; 2019 Jan-. [cited 2019

Sep 10]. Available from: http://www.ncbi.nlm.nih.gov/pubmed/31335063
27. Librepath. File: Retina -- high mag.jpg (CC BY-SA 3.0) [Internet]. Wikimedia Commons. 2015 [cited 2019 Sep 11]. Available from: https://commons.wikimedia.org/wiki/File:Retina_--_high_mag.jpg
28. Purves D, Augustine GJ, Fitzpatrick D, Katz LC, LaMantia A-S, McNamara JO, et al. Neuroscience. [Internet]. 2nd ed. Sunderland (MA): Sinauer Associates; 2001. Phototransduction; [cited 2019 Sep 10]. Available from: https://www.ncbi.nlm.nih.gov/books/NBK10806/
29. Imamoto Y, Shichida Y. Cone visual pigments. Biochim Biophys Acta - Bioenerg [Internet]. 2014 May 1 [cited 2019 Sep 10];1837(5):664–73. Available from: https://www.sciencedirect.com/science/article/pii/S0005272813001461
30. Burgoyne T, Meschede IP, Burden JJ, Bailly M, Seabra MC, Futter CE. Rod disc renewal occurs by evagination of the ciliary plasma membrane that makes cadherin-based contacts with the inner segment. Proc Natl Acad Sci U S A [Internet]. 2015 Dec 29 [cited 2018 Aug 28];112(52):15922–7. Available from: http://www.ncbi.nlm.nih.gov/pubmed/26668363
31. Jan R. File:Schema Retina.jpg (CC BY-SA 2.0 DE) [Internet]. Wikimedia Commons. 2005 [cited 2019 Sep 11]. Available from: https://commons.wikimedia.org/wiki/File:Schema_Retina.jpg
32. Alvord LS, Farmer BL. Anatomy and orientation of the human external ear. J Am Acad Audiol [Internet]. 1997 Dec [cited 2019 Sep 13];8(6):383–90. Available from: https://pdfs.semanticscholar.org/93a9/4c5e4ef8964ecaf19e87dbd2d7e85eccdae0.pdf
33. Sánchez López de Nava A, Lasrado S. Physiology, Ear. [Updated 2019 Apr 27]. In: StatPearls [Internet]. Treasure Island (FL): StatPearls Publishing; 2019 Jan-.; [cited 2019 Sep 13]. Available from: http://www.ncbi.nlm.nih.gov/pubmed/31082036
34. Szymanski A, Toth J, Geiger Z. Anatomy, Head and Neck, Ear Tympanic Membrane. [Updated 2019 Aug 6]. In: StatPearls [Internet]. Treasure Island (FL): StatPearls Publishing; 2019 Jan-; [cited 2019 Sep 14]. Available from: http://www.ncbi.nlm.nih.gov/pubmed/28846242
35. Purves D, Augustine GJ, Fitzpatrick D, Katz LC, LaMantia A-S, McNamara JO, et al., editors. Neuroscience. 2nd edition. [Internet]. Sunderland (MA): Sinauer Associates; 2001; The Otolith Organs: The Utricle and Sacculus. Available from: https://www.ncbi.nlm.nih.gov/books/NBK10792/
36. Purves D, Augustine GJ, Fitzpatrick D, Katz LC, LaMantia A-S, McNamara JO, et al. Neuroscience. 2nd edition. [Internet]. Sunderland (MA): Sinauer Associates; 2001; [cited 2019 Sep 15]. The Inner Ear. Available from: https://www.ncbi.nlm.nih.gov/books/NBK10946/
37. Selva P, Morlier J, Gourinat Y. “Development of a Dynamic Virtual Reality Model of the Inner Ear Sensory System as a Learning and Demonstrating Tool” - Figure 2 Global visualization of the inner ear and zoom on the 3 canals (angular sensors) [Internet]. Modelling and Simulation in Engineering, vol. 2009 [cited 2021 Jan 22]. Available from: https://www.hindawi.com/journals/mse/2009/245606/#copyright
38. Hackney CM, Furness DN. The composition and role of cross links in mechanoelectrical transduction in vertebrate sensory hair cells. J Cell Sci [Internet]. 2013 Apr 15 [cited 2019 Sep 16];126(Pt 8):1721–31. Available from:

http://www.ncbi.nlm.nih.gov/pubmed/23641064
39. Gillespie PG, Müller U. Mechanotransduction by Hair Cells: Models, Molecules, and Mechanisms. Cell [Internet]. 2009 [cited 2019 Sep 16];139(1):33–44. Available from: https://www.ncbi.nlm.nih.gov/pmc/articles/PMC2888516/#R24
40. Mathur P, Yang J. Usher syndrome: Hearing loss, retinal degeneration and associated abnormalities. Biochim Biophys Acta - Mol Basis Dis [Internet]. 2015 Mar 1 [cited 2018 Feb 28];1852(3):406–20. Available from: https://www.sciencedirect.com/science/article/pii/S0925443914003627
41. Reiss K. General Zoology. OpenStax CNX. 26. May 2016 [Internet]. [cited 2019 Sep 17]. 25.4 Hearing and Vestibular Sensation. Available from: http://cnx.org/contents/3e3cd1e8-d940-45a2-b4dd-b2ed865fbfea@1.59
42. Silbernagl S, Despopoulos A, editors. Taschenatlas Physiologie. 8th ed. Stuttgart: Georg Thieme Verlag; 2012. 386–388 p.
43. Chittka L, Brockmann A. Perception Space—The Final Frontier (CC BY 4.0) [Internet]. PLoS Biol. 2005 [cited 2019 Sep 17]. Available from: https://journals.plos.org/plosbiology/article?id=10.1371/journal.pbio.0030137
44. Tsilou ET, Rubin BI, Caruso RC, Reed GF, Pikus A, Hejtmancik JF, et al. Usher syndrome clinical types I and II: Could ocular symptoms and signs differentiate between the two types? Acta Ophthalmol Scand [Internet]. 2002 Apr 1 [cited 2018 Mar 2];80(2):196–201. Available from: http://doi.wiley.com/10.1034/j.1600-0420.2002.800215.x
45. Edwards A, Fishman GA, Anderson RJ, Grover S, Derlacki DJ. Visual Acuity and Visual Field Impairment in Usher Syndrome. Arch Ophthalmol [Internet]. 1998 Feb 1 [cited 2019 Aug 23];116(2):165–8. Available from: http://archopht.jamanetwork.com/article.aspx?doi=10.1001/archopht.116.2.165
46. Haim M. The epidemiology of retinitis pigmentosa in Denmark. Acta Ophthalmol Scand [Internet]. 2002 Feb 12 [cited 2018 Aug 31];80:1–34. Available from: http://doi.wiley.com/10.1046/j.1395-3907.2002.00001.x
47. Galan A, Chizzolini M, Milan E, Sebastiani A, Costagliola C, Parmeggiani F. Good Epidemiologic Practice in Retinitis Pigmentosa: From Phenotyping to Biobanking. Curr Genomics [Internet]. 2011 Jun [cited 2018 Mar 2];12(4):260–6. Available from: http://www.eurekaselect.com/openurl/content.php?genre=article&issn=1389-2029&volume=12&issue=4&spage=260
48. Linder B. Etablierung und Charakterisierung eines Tiermodells für Retinitis pigmentosa. 2012 [cited 2018 Feb 26]; Available from: https://opus.bibliothek.uni-wuerzburg.de/opus4-wuerzburg/frontdoor/deliver/index/docId/6630/file/Linder_Diss_Spleissfaktormangel.pdf
49. Condition, gene, or chromosome summary: National Library of Medicine (US). Genetics Home Reference [Internet]. Bethesda (MD): The Library. 2019 Aug 20. Retinitis Pigmentosa; [reviewed October 2010]. [cited 2019 Aug 23]. Available from: https://ghr.nlm.nih.gov/condition/retinitis-pigmentosa
50. Ferrari S, Di Iorio E, Barbaro V, Ponzin D, Sorrentino FS, Parmeggiani F. Retinitis pigmentosa: genes and disease mechanisms. Curr Genomics [Internet]. 2011 Jun [cited 2018 Mar 2];12(4):238–49. Available from: http://www.ncbi.nlm.nih.gov/pubmed/22131869
51. Bowling B. KANSKIs Klinische Ophtalmologie. Ein systemischer Ansatz. 8th

ed. München: Elsevier GmbH Deutschland; 2017. 634–640 p.
52. Hartong DT, Berson EL, Dryja TP. Retinitis pigmentosa Prevalence and inheritance patterns [Internet]. Vol. 368, www.thelancet.com. 2006 [cited 2018 Sep 6]. Available from: www.ncbi.nlm.nih.gov/
53. Kim R, Strohmayer S, Bauer H. Courtesy of the Department of Ophthalmology, Medical University Graz, Photo laboratory [Internet]. [cited 2019 Sep 12]. Available from: http://e-learning.studmed.unibe.ch/augenheilkunde/systematik/netzhaut/retino_pigmentosa.html
54. Häggström M. File:Fundus photograph of normal left eye.jpg, “Medical gallery of Mikael Häggström 2014” (Public Domain) [Internet]. WikiJournal of Medicine 1 (2). 2012 [cited 2019 Sep 11]. Available from: https://commons.wikimedia.org/wiki/File:Fundus_photograph_of_normal_left_eye.jpg
55. Fahim AT, Daiger SP, Weleber RG. Nonsyndromic Retinitis Pigmentosa Overview. 2000 Aug 4 [Updated 2017 Jan 19] [Internet]. Adam M, Adinger H, Pagon R, Al. E, editors. GeneReviews®. Seattle (WA): University of Washington, Seattle; 1993-2019; [cited 2019 Aug 26]. Available from: https://www.ncbi.nlm.nih.gov/books/NBK1417/
56. Young NM, Mets MB, Hain TC. Early diagnosis of Usher syndrome in infants and children. Am J Otol [Internet]. 1996 Jan [cited 2018 Sep 10];17(1):30–4. Available from: http://www.ncbi.nlm.nih.gov/pubmed/8694131
57. Liu G, Liu X, Li H, Du Q, Wang F. Optical Coherence Tomographic Analysis of Retina in Retinitis Pigmentosa Patients. Ophthalmic Res [Internet]. 2016 [cited 2018 Sep 13];56(3):111–22. Available from: http://www.ncbi.nlm.nih.gov/pubmed/27352292
58. Witkin AJ, Ko TH, Fujimoto JG, Chan A, Drexler W, Schuman JS, et al. Ultra-high resolution optical coherence tomography assessment of photoreceptors in retinitis pigmentosa and related diseases. Am J Ophthalmol [Internet]. 2006 Dec [cited 2018 Sep 13];142(6):945–52. Available from: http://www.ncbi.nlm.nih.gov/pubmed/17157580
59. Yung M, Klufas MA, Sarraf D. Clinical applications of fundus autofluorescence in retinal disease. Int J Retin Vitr [Internet]. 2016 Dec 8 [cited 2018 Sep 10];2(1):12. Available from: http://journalretinavitreous.biomedcentral.com/articles/10.1186/s40942-016-0035-x
60. Williams MA, Moutray TN, Jackson AJ. Uniformity of Visual Acuity Measures in Published Studies. Investig Opthalmology Vis Sci [Internet]. 2008 Oct 1 [cited 2019 Aug 27];49(10):4321. Available from: http://iovs.arvojournals.org/article.aspx?doi=10.1167/iovs.07-0511
61. Spector RH. Visual Fields [Internet]. Walker HK, Hall WD, Hurst JW, editors. Clinical Methods: The History, Physical, and Laboratory Examinations. 3rd edition. Boston: Butterworths: Butterworths; 1990 [cited 2019 Aug 30]. Chapter 116. Available from: http://www.ncbi.nlm.nih.gov/pubmed/21250064
62. Nan W, Migotina D, Wan F, Lou CI, Rodrigues J, Semedo J, et al. Dynamic peripheral visual performance relates to alpha activity in soccer players. Front Hum Neurosci [Internet]. 2014 [cited 2019 Aug 30];8:913. Available from: http://www.ncbi.nlm.nih.gov/pubmed/25426058
63. Broadway DC. Visual field testing for glaucoma - a practical guide. Community eye Heal [Internet]. 2012 [cited 2019 Aug 30];25(79–80):66–70. Available

from: http://www.ncbi.nlm.nih.gov/pubmed/23520423
64. Weiss JN, Levy S. Stem Cell Ophthalmology Treatment Study: bone marrow derived stem cells in the treatment of Retinitis Pigmentosa. Stem cell Investig [Internet]. 2018 [cited 2019 Aug 30];5:18. Available from: http://www.ncbi.nlm.nih.gov/pubmed/30050918
65. Perlman I. The Electroretinogram: ERG. 2001 May 1 [Updated 2007 Jun 27] [Internet]. Kolb H, Fernandez E, Nelson R, editors. Webvision: The Organization of the Retina and Visual System. Salt Lake City (UT): University of Utah Health Sciences Center; 1995-: University of Utah Health Sciences Center; [cited 2019 Aug 31]. Available from: http://www.ncbi.nlm.nih.gov/pubmed/21413407
66. Yin R, Xu Z, Mei M, Chen Z, Wang K, Liu Y, et al. Soft transparent graphene contact lens electrodes for conformal full-cornea recording of electroretinogram. Nat Commun [Internet]. 2018 Dec 13 [cited 2018 Sep 12];9(1):2334. Available from: http://www.nature.com/articles/s41467-018-04781-w
67. Adhi M, Duker JS. Optical coherence tomography--current and future applications. Curr Opin Ophthalmol [Internet]. 2013 May [cited 2018 Sep 13];24(3):213–21. Available from: http://www.ncbi.nlm.nih.gov/pubmed/23429598
68. Fujimoto JG, Pitris C, Boppart SA, Brezinski ME. Optical coherence tomography: an emerging technology for biomedical imaging and optical biopsy. Neoplasia [Internet]. 2000 [cited 2019 Sep 2];2(1–2):9–25. Available from: http://www.ncbi.nlm.nih.gov/pubmed/10933065
69. Gabai A, Veritti D, Lanzetta P. Fundus autofluorescence applications in retinal imaging. Indian J Ophthalmol [Internet]. 2015 May [cited 2019 Sep 3];63(5):406–15. Available from: http://www.ncbi.nlm.nih.gov/pubmed/26139802
70. Sepah YJ, Akhtar A, Sadiq MA, Hafeez Y, Nasir H, Perez B, et al. Fundus autofluorescence imaging: Fundamentals and clinical relevance. Saudi J Ophthalmol Off J Saudi Ophthalmol Soc [Internet]. 2014 Apr [cited 2019 Sep 3];28(2):111–6. Available from: http://www.ncbi.nlm.nih.gov/pubmed/24843303
71. Popović P, Jarc-Vidmar M, Hawlina M. Abnormal fundus autofluorescence in relation to retinal function in patients with retinitis pigmentosa. Graefe's Arch Clin Exp Ophthalmol [Internet]. 2005 Oct 20 [cited 2018 Sep 14];243(10):1018–27. Available from: http://link.springer.com/10.1007/s00417-005-1186-x
72. Sahni JN, Angi M, Irigoyen C, Semeraro F, Romano MR, Parmeggiani F. Therapeutic challenges to retinitis pigmentosa: from neuroprotection to gene therapy. Curr Genomics [Internet]. 2011 Jun [cited 2019 Sep 4];12(4):276–84. Available from: http://www.ncbi.nlm.nih.gov/pubmed/22131873
73. Berson EL, Rosner B, Sandberg MA, Hayes KC, Nicholson BW, Weigel-DiFranco C, et al. A randomized trial of vitamin A and vitamin E supplementation for retinitis pigmentosa. Arch Ophthalmol (Chicago, Ill 1960) [Internet]. 1993 Jun [cited 2018 Dec 1];111(6):761–72. Available from: http://www.ncbi.nlm.nih.gov/pubmed/8512476
74. Senapati S, Gragg M, Samuels IS, Parmar VM, Maeda A, Park PS-H. Effect of dietary docosahexaenoic acid on rhodopsin content and packing in photoreceptor cell membranes. Biochim Biophys Acta - Biomembr [Internet].

2018 Jun 1 [cited 2018 Dec 1];1860(6):1403–13. Available from: https://www.sciencedirect.com/science/article/pii/S000527361830110X?via%3Dihub
75. Kumaran N, Michaelides M, Smith AJ, Ali RR, Bainbridge JWB. Retinal gene therapy. Br Med Bull [Internet]. 2018 Jun 1 [cited 2018 Dec 5];126(1):13–25. Available from: https://academic.oup.com/bmb/article/126/1/13/4916003
76. Approaches To Gene Therapy. Salt Lake City (UT): Genetic Science Learning Center [Internet]. 2012 [cited 2018 Dec 7]. Available from: https://learn.genetics.utah.edu/content/genetherapy/approaches/
77. Dalkara D, Goureau O, Marazova K, Sahel J-A. Let There Be Light: Gene and Cell Therapy for Blindness. Hum Gene Ther [Internet]. 2016 Feb [cited 2018 Dec 3];27(2):134–47. Available from: http://www.ncbi.nlm.nih.gov/pubmed/26751519
78. Help Me Understand Genetics page: National Library of Medicine (US). Genetics Home Reference [Internet]. Bethesda (MD): The Library; 2019 Sep 03. What is gene therapy? [cited 2019 Sep 3]. Available from: https://ghr.nlm.nih.gov/primer/therapy/genetherapy
79. Help Me Understand Genetics page: National Library of Medicine (US). Genetics Home Reference. Bethesda (MD): The Library; 2019 Aug 20. How does gene therapy work?
80. Ameri H. Prospect of retinal gene therapy following commercialization of voretigene neparvovec-rzyl for retinal dystrophy mediated by RPE65 mutation. J Curr Ophthalmol. 2018;30(1):1-2. Published 2018 Feb 16. [Internet]. [cited 2020 Dec 6]. Available from: https://www.ncbi.nlm.nih.gov/pmc/articles/PMC5859497/#idm140321289434944title
81. Zallocchi M, Binley K, Lad Y, Ellis S, Widdowson P, Iqball S, et al. EIAV-based retinal gene therapy in the shaker1 mouse model for usher syndrome type 1B: development of UshStat. PLoS One [Internet]. 2014 [cited 2018 Dec 10];9(4):e94272. Available from: http://www.ncbi.nlm.nih.gov/pubmed/24705452
82. Burnight ER, Gupta M, Wiley LA, Anfinson KR, Tran A, Triboulet R, et al. Using CRISPR-Cas9 to Generate Gene-Corrected Autologous iPSCs for the Treatment of Inherited Retinal Degeneration. Mol Ther [Internet]. 2017 Sep 6 [cited 2019 Feb 5];25(9):1999–2013. Available from: https://www.sciencedirect.com/science/article/pii/S1525001617302332
83. Murken J, Grimm T, Holinski-Feder E, Zerres K, editors. Taschenlehrbuch Humangenetik. 8th ed. Stuttgart: Georg Thieme Verlag; 2011. 8, 244–271 p.
84. Tucker BA, Park I-H, Qi SD, Klassen HJ, Jiang C, Yao J, et al. Transplantation of Adult Mouse iPS Cell-Derived Photoreceptor Precursors Restores Retinal Structure and Function in Degenerative Mice. Nelson B, editor. PLoS One [Internet]. 2011 Apr 29 [cited 2019 Feb 5];6(4):e18992. Available from: https://dx.plos.org/10.1371/journal.pone.0018992
85. Alexander P, Thomson HAJ, Luff AJ, Lotery AJ. Retinal pigment epithelium transplantation: concepts, challenges, and future prospects. Eye (Lond) [Internet]. 2015 Aug [cited 2019 Sep 5];29(8):992–1002. Available from: http://www.ncbi.nlm.nih.gov/pubmed/26043704
86. Schwartz SD, Regillo CD, Lam BL, Eliott D, Rosenfeld PJ, Gregori NZ, et al. Human embryonic stem cell-derived retinal pigment epithelium in patients with age-related macular degeneration and Stargardt's macular dystrophy: follow-

up of two open-label phase 1/2 studies. Lancet [Internet]. 2015 Feb 7 [cited 2019 Sep 5];385(9967):509–16. Available from: https://www.thelancet.com/journals/lancet/article/PIIS0140-6736(14)61376-3/fulltext
87. Seiler MJ, Aramant RB. Cell replacement and visual restoration by retinal sheet transplants. Prog Retin Eye Res [Internet]. 2012 [cited 2019 Sep 5];31(6):661. Available from: https://www.ncbi.nlm.nih.gov/pmc/articles/PMC3472113/
88. National Eye Institute, NIH. How iPSC Works (Public Domain Mark 1.0) [Internet]. NIH image gallery on Flickr. 2018 [cited 2019 Sep 11]. Available from: https://www.flickr.com/photos/nihgov/46181969695/in/album-72157662951050375/
89. Santos A, Humayun MS, de Juan E, Greenburg RJ, Marsh MJ, Klock IB, et al. Preservation of the Inner Retina in Retinitis Pigmentosa. Arch Ophthalmol [Internet]. 1997 Apr 1 [cited 2019 Sep 5];115(4):511. Available from: http://www.ncbi.nlm.nih.gov/pubmed/9109761
90. Dagnelie G. Retinal implants. Curr Opin Neurol [Internet]. 2012 Feb [cited 2019 Sep 5];25(1):67–75. Available from: https://insights.ovid.com/crossref?an=00019052-201202000-00012
91. Zrenner E, Bartz-Schmidt KU, Benav H, Besch D, Bruckmann A, Gabel V-P, et al. Subretinal electronic chips allow blind patients to read letters and combine them to words. Proceedings Biol Sci [Internet]. 2011 May 22 [cited 2019 Sep 7];278(1711):1489–97. Available from: http://www.ncbi.nlm.nih.gov/pubmed/21047851
92. Ho AC, Humayun MS, Dorn JD, da Cruz L, Dagnelie G, Handa J, et al. Long-Term Results from an Epiretinal Prosthesis to Restore Sight to the Blind. Ophthalmology [Internet]. 2015 Aug [cited 2019 Sep 8];122(8):1547–54. Available from: http://www.ncbi.nlm.nih.gov/pubmed/26162233
93. da Cruz L, Coley BF, Dorn J, Merlini F, Filley E, Christopher P, et al. The Argus II epiretinal prosthesis system allows letter and word reading and long-term function in patients with profound vision loss. Br J Ophthalmol [Internet]. 2013 May 1 [cited 2019 Sep 5];97(5):632–6. Available from: http://www.ncbi.nlm.nih.gov/pubmed/23426738
94. Deafness and hearing loss. World Health Organization; 20 March 2019 [Internet]. Licence: CC BY-NC-SA 3.0 IGO. [cited 2020 Jan 1]. Available from: https://www.who.int/news-room/fact-sheets/detail/deafness-and-hearing-loss
95. Koffler T, Ushakov K, Avraham KB. Genetics of Hearing Loss: Syndromic. Otolaryngol Clin North Am [Internet]. 2015 Dec [cited 2018 Mar 14];48(6):1041–61. Available from: http://www.ncbi.nlm.nih.gov/pubmed/26443487
96. Shearer A, Hildebrand M, Smith R. Hereditary Hearing Loss and Deafness Overview. 1999 Feb 14 [Updated 2017 Jul 27]. GeneReviews® [Internet]. Adam M, Ardinger H, Pagon R, Al. E, editors. Seattle (WA): University of Washington, Seattle; 1993-2019.; [cited 2020 Jan 1]. Available from: https://www.ncbi.nlm.nih.gov/books/NBK1434/
97. Korver AMH, Smith RJH, Van Camp G, Schleiss MR, Bitner-Glindzicz MAK, Lustig LR, et al. Congenital hearing loss. Nat Rev Dis Prim. 2017 Jan 12;3.
98. Anastasiadou S, Al Khalili Y. Hearing Loss. [Updated 2020 Jun 5]. In: StatPearls [Internet]. Treasure Island (FL): StatPearls Publishing; 2020 Jan-. [Internet]. [cited 2020 Nov 3]. Available from:

https://www.ncbi.nlm.nih.gov/books/NBK542323/
99. Help Me Understand Genetics page: National Library of Medicine (US). Genetics Home Reference [Internet]. Bethesda (MD): The Library; 2019 Aug 6. What is DNA? [cited 2019 Aug 8]. Available from: https://ghr.nlm.nih.gov/primer/basics/dna
100. Genetic Alliance; The New England Public Health Genetics Education Collaborative. Understanding Genetics: A New England Guide for Patients and Health Professionals [Internet]. Washington (DC): Genetic Alliance; 2010 [cited 2019 Aug 8]. p. Chapter 1, Genetics 101. Available from: https://www.ncbi.nlm.nih.gov/books/NBK132184/
101. Help Me Understand Genetics page: National Library of Medicine (US). Genetics Home Reference [Internet]. Bethesda (MD): The Library; 2019 Aug 6. What is a gene? [cited 2019 Aug 8]. Available from: https://ghr.nlm.nih.gov/primer/basics/gene
102. Reiners J, van Wijk E, Märker T, Zimmermann U, Jürgens K, te Brinke H, et al. Scaffold protein harmonin (USH1C) provides molecular links between Usher syndrome type 1 and type 2. Hum Mol Genet [Internet]. 2005 Dec 15 [cited 2018 Mar 19];14(24):3933–43. Available from: http://academic.oup.com/hmg/article/14/24/3933/2355863/Scaffold-protein-harmonin-USH1C-provides-molecular
103. Splettstoesser T. File:Chromosom-DNA-Gen.png (CC BY 4.0) [Internet]. Wikimedia Commons. 2016 [cited 2019 Sep 11]. Available from: https://commons.wikimedia.org/wiki/File:Chromosom-DNA-Gen.png
104. National Human Genome Research Institute. Autosomal Dominant | Talking Glossary of Genetic Terms | NHGRI [Internet]. [cited 2019 Aug 6]. Available from: https://www.genome.gov/genetics-glossary/Autosomal-Dominant
105. Kashmiri. Based on earlier work of the U.S. National Library of Medicine. File:Autosomal recessive - en.svg (CC BY-SA 3.0). [Internet]. Wikimedia Commons. 2013 [cited 2019 Sep 12]. Available from: https://commons.wikimedia.org/wiki/File:Autosomal_recessive_-_en.svg
106. Ebermann I, Phillips JB, Liebau MC, Koenekoop RK, Schermer B, Lopez I, et al. PDZD7 is a modifier of retinal disease and a contributor to digenic Usher syndrome. J Clin Invest [Internet]. 2010 Jun [cited 2018 Apr 11];120(6):1812–23. Available from: http://www.ncbi.nlm.nih.gov/pubmed/20440071
107. Sun T, Xu K, Ren Y, Xie Y, Zhang X, Tian L, et al. **Comprehensive Molecular Screening in Chinese Usher Syndrome Patients**. Investig Opthalmology Vis Sci [Internet]. 2018 Mar 5 [cited 2018 Aug 3];59(3):1229. Available from: http://iovs.arvojournals.org/article.aspx?doi=10.1167/iovs.17-23312
108. Deltas C. Digenic inheritance and genetic modifiers. Clin Genet [Internet]. 2018 Mar 1 [cited 2018 Aug 3];93(3):429–38. Available from: http://doi.wiley.com/10.1111/cge.13150
109. Sodi A, Mariottini A, Passerini I, Murro V, Tachyla I, Bianchi B, et al. MYO7A and USH2A gene sequence variants in Italian patients with Usher syndrome. Mol Vis [Internet]. 2014 [cited 2018 Aug 3];20:1717–31. Available from: http://www.ncbi.nlm.nih.gov/pubmed/25558175
110. Le P, Stabej Q, Saihan Z, Rangesh N, Steele-Stallard HB, Ambrose J, et al. Comprehensive sequence analysis of nine Usher syndrome genes in the UK National Collaborative Usher Study. [cited 2018 Aug 3]; Available from: http://www.thebsa.org.uk/docs/RecPro/CTP.pdf
111. Help Me Understand Genetics page: National Library of Medicine (US).

Genetics Home Reference [Internet]. Bethesda (MD): The Library; 2019 Aug 6. What is a gene mutation and how do mutations occur? [cited 2019 Aug 11]. Available from: https://ghr.nlm.nih.gov/primer/mutationsanddisorders/genemutation
112. Yourgenome. What types of mutation are there? [Internet]. last updated: 25.01.2016. [cited 2019 Aug 12]. Available from: https://www.yourgenome.org/facts/what-types-of-mutation-are-there
113. Help Me Understand Genetics page: National Library of Medicine (US). Genetics Home Reference [Internet]. Bethesda (MD): The Library; 2019 Aug 6. What kinds of gene mutations are possible? [cited 2019 Aug 12]. Available from: https://ghr.nlm.nih.gov/primer/mutationsanddisorders/possiblemutations
114. Genome Research Limited. What types of mutation are there? | Facts | yourgenome.org (CC BY 3.0) [Internet]. 2016 [cited 2019 Sep 12]. Available from: https://www.yourgenome.org/facts/what-types-of-mutation-are-there
115. Murken J, Grimm T, Holinski-Feder E, Zerres K, editors. Taschenlehrbuch Humangenetik. 8th ed. Stuttgart: Georg Thieme Verlag; 2011. 49–60 p.
116. Point mutation | Talking Glossary of Genetic Terms | NHGRI (Public Domain) [Internet]. National Human Genome Research Institute (genome.gov). [cited 2019 Sep 12]. Available from: https://www.genome.gov/genetics-glossary/Point-Mutation
117. Help Me Understand Genetics page: National Library of Medicine (US). Genetics Home Reference [Internet]. Bethesda (MD): The Library; 2019 Aug 6. What are whole exome sequencing and whole genome sequencing? [cited 2019 Aug 15]. Available from: https://ghr.nlm.nih.gov/primer/testing/sequencing
118. Wallace SE, Bean LJ. Educational Materials — Genetic Testing: Current Approaches. 2017 Mar 14 [Updated 2018 Feb 12]. In: Adam MP, Ardinger HH, Pagon RA, et al., editors. GeneReviews® [Internet]. Seattle (WA): University of Washington, Seattle; 1993-2019; [cited 2019 Aug 15]. Available from: https://www.ncbi.nlm.nih.gov/books/NBK279899/#app5.Multigene_Panels
119. Dilliott AA, Farhan SMK, Ghani M, Sato C, Liang E, Zhang M, et al. Targeted Next-generation Sequencing and Bioinformatics Pipeline to Evaluate Genetic Determinants of Constitutional Disease. J Vis Exp [Internet]. 2018 [cited 2019 Aug 16];(134). Available from: http://www.ncbi.nlm.nih.gov/pubmed/29683450
120. Help Me Understand Genetics page: National Library of Medicine (US). Genetics Home Reference [Internet]. Bethesda (MD): The Library; 2019 Aug 6. What are the risks and limitations of genetic testing? [cited 2019 Aug 16]. Available from: https://ghr.nlm.nih.gov/primer/testing/riskslimitations
121. Usher syndrome - Phenotypic Series - PS276900. [Internet]. Online Mendelian Inheritance in Man, OMIM (TM). McKusick-Nathans Institute of Genetic Medicine, Johns Hopkins University (Baltimore, MD) and National Center for Biotechnology Information, National Library of Medicine (Bethesda, MD). [cited 2019 Aug 17]. Available from: https://www.omim.org/phenotypicSeries/PS276900
122. Wang Y, Li J, Yao X, Li W, Du H, Tang M, et al. Loss of CIB2 Causes Profound Hearing Loss and Abolishes Mechanoelectrical Transduction in Mice. Front Mol Neurosci [Internet]. 2017 Dec 4 [cited 2018 Mar 18];10:401. Available

from: http://journal.frontiersin.org/article/10.3389/fnmol.2017.00401/full
123. Ahmed Z, Riazuddin S, Khan S, Friedman P, Riazuddin S, Friedman T. USH1H, a novel locus for type I Usher syndrome, maps to chromosome 15q22-23. Clin Genet [Internet]. 2009 Jan 1 [cited 2019 Aug 19];75(1):86–91. Available from: http://doi.wiley.com/10.1111/j.1399-0004.2008.01038.x
124. Jaworek TJ, Bhatti R, Latief N, Khan SN, Riazuddin S, Ahmed ZM. USH1K, a novel locus for type I Usher syndrome, maps to chromosome 10p11.21–q21.1. J Hum Genet [Internet]. 2012 Oct 21 [cited 2019 Aug 19];57(10):633–7. Available from: http://www.nature.com/articles/jhg201279
125. Chaib H, Kaplan J, Gerber S, Vincent C, Ayadi H, Slim R, et al. A newly identified locus for Usher syndrome type I, USH1E, maps to chromosome 21q21. Hum Mol Genet [Internet]. 1997 Jan 1 [cited 2019 Aug 19];6(1):27–31. Available from: https://academic.oup.com/hmg/article-lookup/doi/10.1093/hmg/6.1.27
126. Gerber S, Bonneau D, Gilbert B, Munnich A, Dufier J-L, Rozet J-M, et al. USH1A: chronicle of a slow death. Am J Hum Genet [Internet]. 2006 Feb [cited 2018 Nov 23];78(2):357–9. Available from: http://www.ncbi.nlm.nih.gov/pubmed/16400615
127. Williams DS, Lopes VS. The many different cellular functions of MYO7A in the retina. Biochem Soc Trans [Internet]. 2011 Oct [cited 2018 Feb 26];39(5):1207–10. Available from: http://www.ncbi.nlm.nih.gov/pubmed/21936790
128. Williams DS. Usher syndrome: animal models, retinal function of Usher proteins, and prospects for gene therapy. Vision Res [Internet]. 2008 Feb [cited 2018 Mar 2];48(3):433–41. Available from: http://www.ncbi.nlm.nih.gov/pubmed/17936325
129. Hata Y, Iida J. Scaffold Protein. In: Binder MD, Hirokawa N, Windhorst U, editors. Encyclopedia of Neuroscience [Internet]. Berlin, Heidelberg: Springer Berlin Heidelberg; 2009. p. 3613–6. Available from: https://doi.org/10.1007/978-3-540-29678-2_5231
130. Lee H-J, Zheng JJ. PDZ domains and their binding partners: structure, specificity, and modification. Cell Commun Signal [Internet]. 2010 May 28 [cited 2018 Mar 19];8:8. Available from: http://www.ncbi.nlm.nih.gov/pubmed/20509869
131. Boëda B, El-Amraoui A, Bahloul A, Goodyear R, Daviet L, Blanchard S, et al. Myosin VIIa, harmonin and cadherin 23, three Usher I gene products that cooperate to shape the sensory hair cell bundle. EMBO J [Internet]. 2002 Dec 16 [cited 2018 Mar 19];21(24):6689–99. Available from: http://www.ncbi.nlm.nih.gov/pubmed/12485990
132. Reiners J, Reidel B, El-Amraoui A, Boe¨da B, Huber I, Petit C, et al. Differential Distribution of Harmonin Isoforms and Their Possible Role in Usher-1 Protein Complexes in Mammalian Photoreceptor Cells. Investig Opthalmology Vis Sci [Internet]. 2003 Nov 1 [cited 2018 Mar 19];44(11):5006. Available from: http://iovs.arvojournals.org/article.aspx?doi=10.1167/iovs.03-0483
133. Doucette L, Merner ND, Cooke S, Ives E, Galutira D, Walsh V, et al. Profound, prelingual nonsyndromic deafness maps to chromosome 10q21 and is caused by a novel missense mutation in the Usher syndrome type IF gene PCDH15. Eur J Hum Genet [Internet]. 2009 May [cited 2018 Mar 25];17(5):554–64. Available from: http://www.ncbi.nlm.nih.gov/pubmed/19107147

134. Jacoszek A, Pollak A, Płoski R, Ołdak M. Advances in genetic hearing loss: CIB2 gene. Eur Arch Oto-Rhino-Laryngology [Internet]. 2017 Apr 22 [cited 2018 Mar 18];274(4):1791–5. Available from: http://link.springer.com/10.1007/s00405-016-4330-9
135. van Wijk E, Pennings RJE, te Brinke H, Claassen A, Yntema HG, Hoefsloot LH, et al. Identification of 51 novel exons of the Usher syndrome type 2A (USH2A) gene that encode multiple conserved functional domains and that are mutated in patients with Usher syndrome type II. Am J Hum Genet [Internet]. 2004 Apr [cited 2018 Apr 8];74(4):738–44. Available from: http://www.ncbi.nlm.nih.gov/pubmed/15015129
136. Liu X, Bulgakov O V, Darrow KN, Pawlyk B, Adamian M, Liberman MC, et al. Usherin is required for maintenance of retinal photoreceptors and normal development of cochlear hair cells. Proc Natl Acad Sci U S A [Internet]. 2007 Mar 13 [cited 2018 Apr 7];104(11):4413–8. Available from: http://www.ncbi.nlm.nih.gov/pubmed/17360538
137. Michalski N, Michel V, Bahloul A, Lefèvre G, Barral J, Yagi H, et al. Molecular characterization of the ankle-link complex in cochlear hair cells and its role in the hair bundle functioning. J Neurosci [Internet]. 2007 Jun 13 [cited 2018 Apr 10];27(24):6478–88. Available from: http://www.ncbi.nlm.nih.gov/pubmed/17567809
138. Zou J, Lee A, Yang J. The expression of whirlin and Cav1.3α_1 is mutually independent in photoreceptors. Vision Res [Internet]. 2012 Dec 15 [cited 2018 Apr 9];75:53–9. Available from: http://www.ncbi.nlm.nih.gov/pubmed/22892111
139. Zou J, Luo L, Shen Z, Chiodo VA, Ambati BK, Hauswirth WW, et al. Whirlin replacement restores the formation of the USH2 protein complex in whirlin knockout photoreceptors. Invest Ophthalmol Vis Sci [Internet]. 2011 Apr [cited 2018 Apr 9];52(5):2343–51. Available from: http://www.ncbi.nlm.nih.gov/pubmed/21212183
140. Chen Q, Zou J, Shen Z, Zhang W, Yang J. Whirlin and PDZ domain-containing 7 (PDZD7) proteins are both required to form the quaternary protein complex associated with Usher syndrome type 2. J Biol Chem [Internet]. 2014 Dec 26 [cited 2018 Apr 11];289(52):36070–88. Available from: http://www.ncbi.nlm.nih.gov/pubmed/25406310
141. Vona B, Lechno S, Hofrichter MAH, Hopf S, Läig AK, Haaf T, et al. Confirmation of PDZD7 as a Nonsyndromic Hearing Loss Gene. Ear Hear [Internet]. 2016 [cited 2018 Apr 11];37(4):e238–46. Available from: http://www.ncbi.nlm.nih.gov/pubmed/26849169
142. RetNet: Disease Table [Internet]. [cited 2018 Apr 9]. Available from: https://sph.uth.edu/retnet/disease.htm
143. Dinculescu A, Stupay RM, Deng W-T, Dyka FM, Min S-H, Boye SL, et al. AAV-Mediated Clarin-1 Expression in the Mouse Retina: Implications for USH3A Gene Therapy. PLoS One [Internet]. 2016 [cited 2018 Apr 13];11(2):e0148874. Available from: http://www.ncbi.nlm.nih.gov/pubmed/26881841
144. Cosgrove D, Zallocchi M. Clarin-1 protein expression in photoreceptors. Hear Res [Internet]. 2010 Jan [cited 2018 Apr 15];259(1–2):117. Available from: http://www.ncbi.nlm.nih.gov/pubmed/19772908
145. Ogun O, Zallocchi M. Clarin-1 acts as a modulator of mechanotransduction activity and presynaptic ribbon assembly. J Cell Biol [Internet]. 2014 Nov 10

[cited 2018 Apr 13];207(3):375–91. Available from: http://www.ncbi.nlm.nih.gov/pubmed/25365995
146. Liu XZ, Hope C, Walsh J, Newton V, Ke XM, Liang CY, et al. Mutations in the myosin VIIA gene cause a wide phenotypic spectrum, including atypical Usher syndrome. Am J Hum Genet [Internet]. 1998 Sep 1 [cited 2018 Jul 31];63(3):909–12. Available from: http://www.ncbi.nlm.nih.gov/pubmed/9718356
147. Bashir R, Fatima A, Naz S. A frameshift mutation in SANS results in atypical Usher syndrome. Clin Genet [Internet]. 2010 Dec [cited 2018 Jul 31];78(6):601–3. Available from: http://www.ncbi.nlm.nih.gov/pubmed/21044053
148. Cremers FPM, Kimberling WJ, Külm M, de Brouwer AP, van Wijk E, te Brinke H, et al. Development of a genotyping microarray for Usher syndrome. J Med Genet [Internet]. 2007 Feb 1 [cited 2018 Jul 31];44(2):153–60. Available from: http://www.ncbi.nlm.nih.gov/pubmed/16963483
149. Mataftsi A, Koutsimpogeorgos D, Brazitikos P, Ziakas N, Haidich A. Is conversion of decimal visual acuity measurements to logMAR values reliable? Graefes Arch Clin Exp Ophthalmol. 2019 Jul;257(7):1513-1517. [Internet]. Available from: https://pubmed.ncbi.nlm.nih.gov/31069515/#:~:text=Decimal scores were converted to,-log(decimal acuity).
150. Sachsenweger Ma. Duale Reihe - Augenheilkunde, 2. vollständig überarbeitete und erweiterte Auflage. Georg Thieme Verlag; 2003. 362 p.
151. World Health Organization. International classification of diseases for mortality and morbidity statistics (10th Revision) [Internet]. 2020 [cited 2020 Nov 28]. Available from: https://icd.who.int/browse10/2019/en#/H54.9
152. Mingui K, Da Ye C, Gyule H, Yun-Mi S, Sung Yong P, Joohon S, et al. Measurable Range of Subfoveal Choroidal Thickness With Conventional Spectral Domain Optical Coherence Tomography [Internet]. translational vision science & technology an ARVO journal, September 2018, Volume 7, Issue 5. 2018 [cited 2020 Nov 28]. Available from: https://tvst.arvojournals.org/article.aspx?articleid=2705524
153. National Center for Biotechnology Information. ClinVar [Internet]. [cited 2020 Nov 29]. Available from: https://www.ncbi.nlm.nih.gov/clinvar/
154. Richards S, Aziz N, Bale S, Al E. Standards and guidelines for the interpretation of sequence variants: a joint consensus recommendation of the American College of Medical Genetics and Genomics and the Association for Molecular Pathology. Genet Med 17, 405–423 [Internet]. 2015 [cited 2020 Nov 29]. Available from: https://www.nature.com/articles/gim201530
155. Blanco-Kelly F, Jaijo T, Aller E, Avila-Fernandez A, López-Molina MI, Giménez A, et al. Clinical Aspects of Usher Syndrome and the *USH2A* Gene in a Cohort of 433 Patients. JAMA Ophthalmol [Internet]. 2015 Feb 1 [cited 2018 Feb 26];133(2):157. Available from: http://archopht.jamanetwork.com/article.aspx?doi=10.1001/jamaophthalmol.2014.4498
156. Rangaswamy VN, Patel HM, Locke KG, Hood DC, Birch DG. A Comparison of Visual Field Sensitivity to Photoreceptor Thickness in Retinitis Pigmentosa. Invest. Ophthalmol. Vis. Sci. 2011;52(1):101-108. [Internet]. [cited 2020 Dec 1]. Available from: https://www.ncbi.nlm.nih.gov/pmc/articles/PMC2910646/pdf/z7g4213.pdf
157. Colombo L, Sala B, Montesano G, Pierrottet C, De Cillà S, Maltese P, et al.

Choroidal Thickness Analysis in Patients with Usher Syndrome Type 2 Using EDI OCT. Journal of Ophthalmology, vol. 2015, Article ID 189140, 6 pages, 2015 [Internet]. 2015 [cited 2020 Dec 1]. Available from: https://www.hindawi.com/journals/joph/2015/189140/

158. Sabbaghi H, Ahmadieh H, Jalili J, Behnaz N, Fakhri M, Suri F, et al. Choroidal Thickness in Different Types of Inherited Retinal Dystrophies. Journal of ophthalmic & vision research, 15(3), 351–361. [Internet]. 2020 [cited 2020 Dec 1]. Available from: https://www.ncbi.nlm.nih.gov/pmc/articles/PMC7431727/